

Design and Optimization of Spiral Cladding Photonic Crystal Fibre Based Sensor for Gas Sensing Applications

A Project Report

Submitted in partial fulfillment of the requirement for the award of the degree of

Bachelor of Technology *in* **Electronics and Communication Engineering**

by

KUMARAJEEVA E

14BEC0248

Under the guidance of

Prof. REVATHI. S

Associate professor

School of Electronics Engineering

Vellore Institute of Technology, Vellore-632014



VIT[®]
Vellore Institute of Technology
(Deemed to be University under section 3 of UGC Act, 1956)

April 2018

DECLARATION

I hereby declare that the project work entitled “**Design and Optimization of Spiral Cladding Photonic Crystal Fibre Based Sensor for Gas Sensing Applications**” submitted by me, for the award of the degree of *Bachelor of Technology in Electronics and Communication Engineering* to Vellore Institute of Technology is a record of bonafide work carried out by me under the supervision of **REVATHI. S**

I further declare that the work reported in this report has not been submitted and will not be submitted, either in part or in full, for the award of any other degree or diploma in this institute or any other institute or university.

Place : Vellore

Signature of the Candidate

Date :21/04/2018

Kumarajeeva.E
(14BEC0248)

CERTIFICATE

This is to certify that the project work entitled “**Design and Analysis of Photonic Crystal Fiber as Gas Sensor**” submitted by **KUMARAJEEVA E**, School of Electronics Engineering, Vellore Institute of Technology, for the award of the degree of *Bachelor of Technology in Electronics and Communication Engineering*, is a record of bonafide work carried out by him/her under my supervision, as per the VIT code of academic and research ethics.

The contents of this report have not been submitted and will not be submitted either in part or in full, for the award of any other degree or diploma in this institute or any other institute or university. The report fulfills the requirements and regulations of the institute and in my opinion meets the necessary standards for submission.

Place : Vellore

Date : 21/04/2018

Signature of the Guide

Dr. Revathi.S

The project work is satisfactory / unsatisfactory

Internal Examiner

External Examiner

Approved by

Head of the Department
Department of Communication Engineering

ACKNOWLEDGEMENT

I would like to start by thanking **VIT University, Chancellor of VIT , Vice Chancellor of VIT**. From the first day to the last, they have been present all along, in the form of opportunities at every step, and their innovation, infused deep within the fabric of university life.

In the light of recent developments and project progress, several factors have contributed toward the path of project completion. Each of these factors has provided support and feedback in their own way, with the nature of extended support ranging from simple feedback and assurance, to provision of actual details and periodic updates on the exact status of the project.

Thus, I would like to thank my guide, **Prof. Revathi S**, for all her timely advice, feedback, and acknowledgement for various project requirements. She has been exemplary in doing all that a project guide should do, irrespective of the time of day, or the extent of short notice availability. . She not only provided me with valuable insights but also portrayed the right scenarios before me. She also helped me in better understanding of various project topics.

In continuation, I would also like to thanking, **HoD, SENSE** for the timely dispatch and updates regarding project guidelines, details, and requirements. Her periodic information releases have surely gone a long way in helping not just me, but the remainder of the project batch in planning their tasks and work flow schedule, thereby maintaining a healthy balance between regular work and project tasks.

In extension of the ongoing presentation of gratitude to various benefactors, a round of acknowledgement is also due for **Dr Elizabeth Rufus., (Dean, SENSE)**. Her steadfast approach to problems and tasks in general, accompanied by her staunch and unyielding leadership have made a mark on all things scope.

Kumarajeeva E

14BEC0248

EXECUTIVE SUMMARY

The development of highly-sensitive and miniaturized sensors that capable of realtime analytes detection is highly desirable. Nowadays, toxic or colourless gas detection, air pollution monitoring, harmful chemical, pressure, strain, humidity, and temperature sensors based on photonic crystal fibre (PCF) are increasing rapidly due to its compact structure, fast response and efficient light controlling capabilities. The propagating light through the PCF can be controlled by varying the structural parameters and as a result, evanescent field can be enhanced significantly which is the main component of the PCF based gas sensors. All the numerical parameters like diameters and pitches of both center and cladding in spiral Photonic Crystal Fibre (S-PCF) have been shifted with an advanced structure. Using Finite Element Method (FEM), it can be secured that the proposed S-PCF demonstrates high relative sensitivity and low confinement loss. The aim of this chapter is to describe the principle operation of S-PCF based gas sensors and to discuss the important properties of the sensor. The investigated results of relative sensitivity and confinement loss are extensively discussed for the different core and cladding shapes and the main challenges of S-PCF based gas sensors and possible solutions are highlighted.

CONTENTS		Page No.
	Acknowledgement	4
	Executive Summary	5
	Table of Contents	6
	List of Figures	8
	List of Tables	10
	List of Terms and Abbreviations	10
	List of Symbols and Notations	11
1	INTRODUCTION	12
	1.1 Motivation	12
	1.2 Background	13
	1.3 Objective	13
	1.4 Organization of the report	33
2	PROJECT DESCRIPTION AND GOALS	34
3	TECHNICAL SPECIFICATION	36
4	DESIGN APPROACH AND DETAILS	41
	4.1 Design Approach	41
	4.2 Codes and Standards	46
	4.3 Constraints, Alternatives and Trade-offs	46
5	SCHEDULE, TASKS AND MILESTONES	48
6	PROJECT DEMONSTRATION	49

7	COST ANALYSIS	58
8	CONCLUSION	59
9	REFERENCES	60

List of Figures:

FIGURE NO	TITLE	PAGE NO.
1.1	Schematic Representation of PCF	13
1.2	Periodic variations in photonic crystal fiber	14
1.3	Typical fabrication process in a photonic crystal fiber.	16
1.4	The fiber drawing tower for PCF fabrication	17
1.5	Photonic crystal fiber fabrication process	17
1.6	Fabrication of photonic crystal fibers: preforms, intermediate preforms and final	19
1.7	Defects in PCF fabrication	20
1.8	Index-Guiding Fibers	21
1.9	Solid Core PCF	22
1.10	Photonic Bandgap Fibers	23
1.11	Hollow core PCF	24
2.1	Schematic of a typical wave-equation problem	35
2.2	PML region surrounding the waveguide structure	36
3.1	Design of a hexagonal PCF in COMSOL	39
3.2	Modal Analysis of PCF	39
3.3	Power confinement shown in COMSOL window for a spiral PCF	40
4.1	Schematic of the proposed S-PCF	41
4.2	Enhanced core of S-PCF	42
4.3	Built Mesh of the proposed S-PCF	44
4.4	Power confinement for fundamental mode of a spiral PCF	45
4.5 (a)	E field for fundamental x mode	45
4.5 (b)	E field for fundamental y mode	46
6.1	Relative sensitivity for a spiral PCF	50
6.2	Confinement loss versus wavelength curve of the proposed S-PCF	51
6.3	V_{eff} vs wavelength for S-PCF	51

6.4	A_{eff} and non linearity versus wavelength	52
6.5	Relative sensitivity versus wavelength for the proposed S-PCF for the variation of filling ratio of the core	54
6.6	Relative sensitivity versus wavelength for the proposed S-PCF for variations of d_1/Λ as 0.45, 0.43 and 0.47	54
6.7	Relative sensitivity versus wavelength for the proposed S-PCF for variations of d_2/Λ as 0.52, 0.50 and 0.54	56
6.8	Relative sensitivity versus wavelength for the proposed S-PCF for the variations of d_3/Λ as 0.6, 0.58 and 0.62	56
6.9	Confinement loss versus wavelength curve of the proposed S-PCF for optimized parameters: $\Lambda = 1.3455 \mu\text{m}$; $\Lambda_c = 0.395 \mu\text{m}$; $d_c = 0.376 \mu\text{m}$; $d/\Lambda = 0.92, 0.94, 0.90$	57

List of Tables:

TABLE NO.	TITLE	PAGE NO
1.1	HISTORY OF PCF	34

List of Terms and Abbreviations:

- PCF** - Photonic Crystal Fiber
- S-PCF** - Spiral shaped Photonic Crystal Fiber
- FEM** - Finite Element Method
- TIR** - Total Internal Reflection
- CP** - Circular Pattern
- NA** - Numerical Aperture
- NL** - Non-Linearity
- PBG** - Photonic Band Gap
- PML** - Perfectly Matched Layer
- TIR** - Total internal reflection
- SMF** - Single Mode photonic fiber
- MMF** - Multimode Photonic fiber

List of Symbols and Notations:

Λ	Pitch of cladding
r_0	Distance of the first air hole in each spiral ring
D_{core}	Diameter of the core
d_c	Diameter of air holes in the center
θ_n	Angular displacement
N	Number of circular rings
Λ_c	Pitch of core
d_c/Λ_c	Air filling ratio of core

1. INTRODUCTION

A sensor is a device, module, or subsystem whose purpose is to detect events or changes in its environment and send the information to other electronics, frequently a computer processor. A gas detector or gas detector is a device that detects the presence of gases in an area, mostly as part of a safety system. This type of equipment is used to detect a gas leak or other emissions and can interface with a control system so a process can be automatically shut down. A gas detector can sound an alarm to operators in the area where the leak is occurring, giving them the opportunity to leave. This type of device is important because there are many gases that can be harmful to organic life, such as humans or animals.

1.1. MOTIVATION

There is a growing interest in developing compact and real time sensors for gas detection. Air quality monitoring often includes the detection of explosive, toxic, and hydrocarbon gases. At present, most of the gas sensing techniques tend to be bulky, expensive, and lack real-time data measurement. Thus, alternative sensing methods are in great demand.

The advancement of telecommunication and non-telecommunication sectors depends on modernizing variant of optical fiber which is renowned as photonic crystal fiber (PCF). It has guaranteed a revolutionary change in fiber optic communication [1]. Day by day PCFs have become too much admired by researchers and forerunner due to its robustness and flexibility. Photonic crystal fibers have received considerable attention as a promising tool for a variety of applications such as telecommunication and supercontinuum generation due to their unique characteristics of the endless single mode, high nonlinearity. In particular, due to the holey structure of PCFs, with holes running along the length of the optical fiber; they have proved their potential to the field of fiber optic chemical and gas sensing. Currently, gas sensors are used to observe the air quality of our environment and discerning of explosive, noxious and hydrocarbon gases.

In addition, industrial safety management purpose like oil and gas production systems are also required gas sensors to detect combustible or toxic gases leakage [2]. a spiral shape photonic crystal fiber (S-PCF) has been suggested as a gas sensor for detecting toxic or colourless gases as well as monitoring the air pollution by metering gas condensate elements in production facilities.

1.2. BACKGROUND

In the last decade, photonic crystal fibers have been under intensive study due to their unique and useful optical properties. PCFs fall into two basic categories. The first one, an index guiding PCF is usually formed by a central solid defect region surrounded by multiple air holes in a regular triangular lattice and confines light by total internal reflection like standard fibers. The second one uses a perfect periodic structure exhibiting a photonic band-gap (PBG) effect at the operating wavelength to guide light in a low index core region, which is also called PBG fiber (PBGF). A typical cross section of a index guiding PCF is shown in Fig 1.1

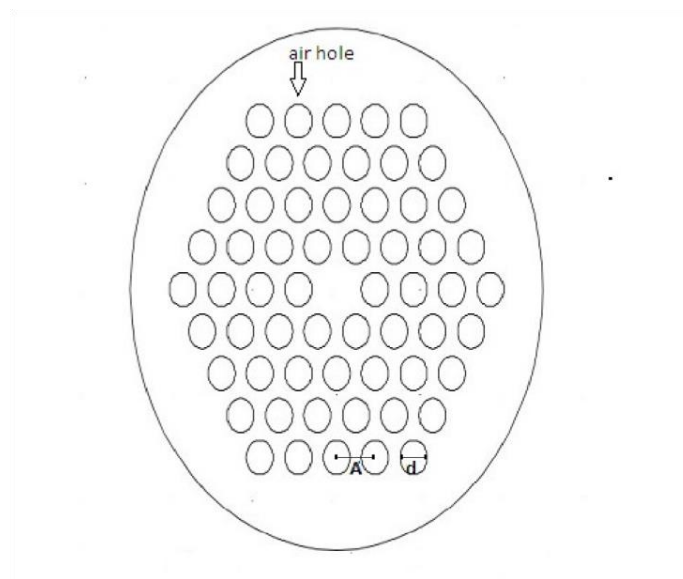


Fig 1.1. Schematic Representation of PCF

1.2.1. Features of a photonic crystal

- Made of low-loss periodic dielectric medium
- Optical analog to the electrical semiconductors
- Able to localize light in specified areas by preventing light from propagating in certain directions – optical bandgap.
- PCFs can be of different structures. They are one dimensional, two dimensional and three dimensional. This variation is shown in Fig 1.2.

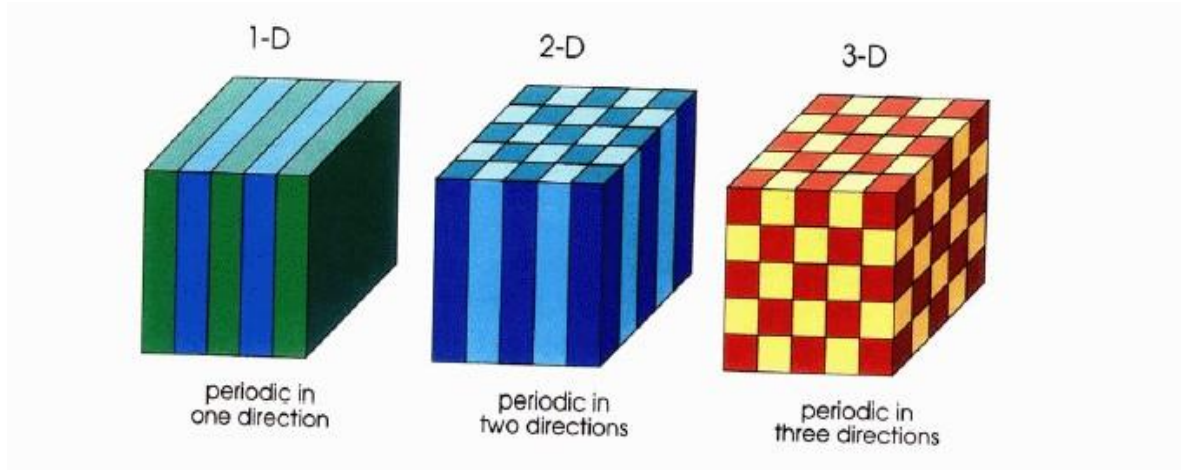


Fig 1.2. Periodic variations in photonic crystal fiber

1.2.2 BASIC EQUATIONS

Propagation of light in PCFs is described by Maxwell's equations. For no free charge or current the following equations become applicable:

$$\nabla \cdot D = 0 \quad (1.1)$$

$$\nabla \times H = \frac{\partial D}{\partial t} \quad (1.2)$$

$$\nabla \cdot B = 0 \quad (1.3)$$

$$\nabla \times E = -\frac{\partial B}{\partial t} \quad (1.4)$$

Restrict to linear low loss media with no frequency dependence of dielectric function such that the following equations become true:

$$\varepsilon(r, \omega) = \varepsilon(r) \in \mathbb{R} \quad (1.5)$$

$$D(r) = \varepsilon(r) \times \varepsilon_0 \times E(r) \quad (1.6)$$

$$B = \mu_0 \cdot H \quad (1.7)$$

Inserting equations (1.5, 1.6, 1.7) in equations (1.1, 1.2, 1.3, 1.4) we get

$$\nabla \cdot \varepsilon(r) \times \varepsilon_0 \times E(r, t) = 0 \quad (1.8)$$

$$\nabla \times H(r, t) = \varepsilon(r) \times \varepsilon_0 \times \frac{\partial E(r, t)}{\partial t} \quad (1.9)$$

$$\nabla \cdot \mu_0 \cdot H(r, t) = 0 \quad (1.10)$$

$$\nabla \times E(r, t) = -\mu_0 \cdot \frac{\partial H(r, t)}{\partial t} \quad (1.11)$$

Since Maxwell's equations are linear we can separate out the time dependence by expanding into a set of harmonic modes,

$$H(r, t) = H(r) \cdot e^{j\omega t} \quad (1.12)$$

$$E(r, t) = E(r) \cdot e^{j\omega t} \quad (1.13)$$

To obtain coupled equations we need the following ones:

$$\nabla \cdot \varepsilon(r) \cdot E(r) = 0 \quad (1.14)$$

$$\nabla \times H(r, t) = j\omega \cdot \varepsilon(r) \varepsilon_0 E(r) \quad (1.15)$$

$$\nabla \cdot H(r) = 0 \quad (1.16)$$

$$\nabla \times E(r) = j\omega \cdot \mu_0 \cdot H(r) \quad (1.17)$$

Decoupling by dividing the dielectric function and taking curl yields

$$\nabla \times \left(\frac{1}{\varepsilon(r)} \nabla \times H(r) \right) = \left(\frac{\omega}{c} \right)^2 \cdot H(r) \quad (1.18)$$

This is the master equation that completely determines the modes $H(r)$ together with the transversality requirement for a given frequency. There are many different methods to solve eigen value problem, but so far all methods rely on numerical calculations.

1.2.3 Fabrication

Photonic crystal fibers are made by stacking tubes and rods of silica glass into a large structure of the pattern of holes required in the final fiber. The perform is then bound with tantalum wire and then is taken to a furnace of fiber drawing tower [3]. The furnace is filled with argon and reach temperature about 2000 as consequence the glass rods and tubes get

soften. Later, the preform is fused together and reduced to 1mm size with hole around 0.05 mm diameter. In other words by increasing the furnace temperature the air hole size can be reduced. After reducing the preform to a size that is 20 times smaller the structure thus formed (cane), the hole process is repeated and spaces between the holes of 25 millionth of meter can be obtained. Defects are created by replacing tubes for solid rods (as in the case of highly nonlinear PCF or by removing a group of tubes from the preform (hollow core photonic PCF). Since the fabrication process is quite robust complicated geometries can be achieved. For instance the geometry of the center defect can be modified by the introduction of the thicker or thinner tubes at different position around the defect [2]. Photonic Crystal Fibers PCF's are devices in which the cladding of the conventional fiber was swapped with photonic structure. This structures are most two dimensional, in which the cladding is an array of microscopic rods of a material of different refraction index, in most of cases it is a hole filled with air, that run along the entire fiber length.

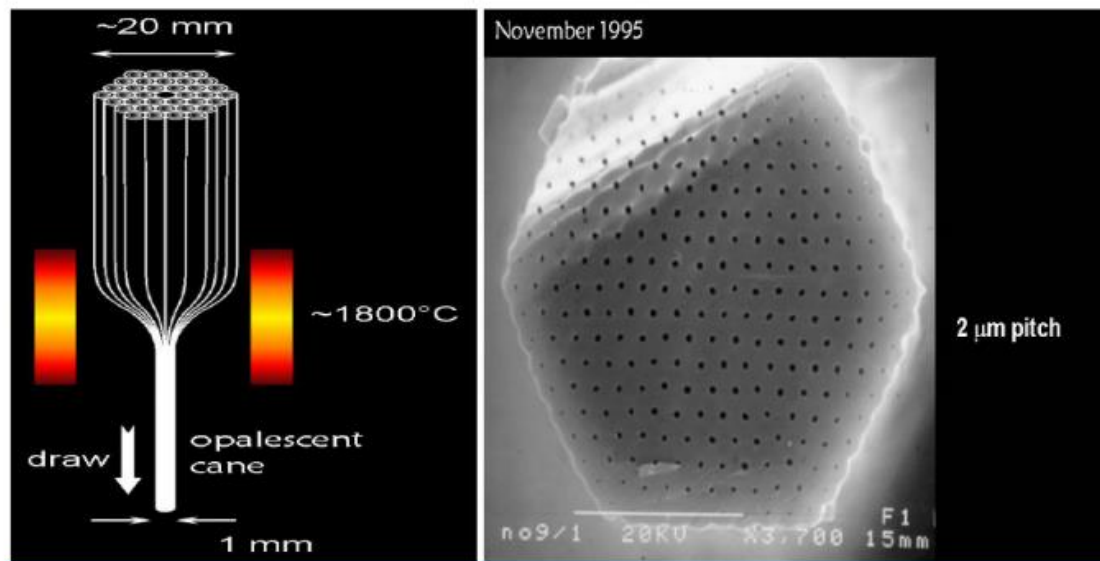


Fig 1.3. Typical fabrication process in a photonic crystal fiber. The tub and rods are gather together and a furnace is used to heat the preform. The preform then fused together reducing its original size with a typical ratio of about 20 [2].



Fig 1.4. The fiber drawing tower for PCF fabrication at the Institute of Electronic Materials Technology, Warsaw, Poland.

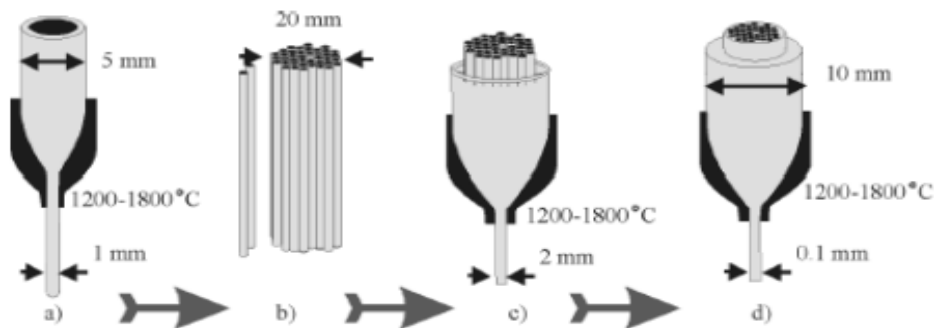


Fig 1.5. Photonic crystal fiber fabrication: (a) creation of individual capillaries, (b) formation of the preform, (c) drawing of intermediate preform, (d) drawing of the final fiber [4].

There are also one dimensional structures of the cladding – in this case the fiber is called Bragg PCF, through analogy with Bragg mirror. The process of fabrication of the PCF is very complicated. Whatever the type of glass and the type of structure, the principal method of fabrication of photonic crystal fibers is multiple thinning. However, there are also reports on fabrication of PCF with extrusion processes, which is mainly used for soft glass PCF formation. In this method, molten glass is forced through a die Containing a designed pattern of holes . The multiple thinning method is well known in the technology of image-guiding

structures performance (fiber plates, image guides, etc.) (Fig 1.4)..With this method, PCFs are fabricated in a several step process (Fig 1.5). In the first step individual capillaries are created. One can use capillaries with different diameters and wall thickness (this influences the d/Λ ratio in the fiber), different cross-sections (circular, hexagonal, square) and different types of glass (silica, silicate, multi-component with various composition of oxides etc.) (Fig 1.6). Next, individual capillaries are positioned, by hand, to make a multi-capillary preform with the required symmetry. The defect in which light propagates is a glass rod or, in the case of fibers with a photonic band gap, a hole with a suitable diameter. These defect rods are positioned in the structure.

A structure so prepared is then fused and drawn with a fiber drawing tower to a millimeter scale and usually named an intermediate preform. This is a thermally integrated glass rod with holes at the locations of the capillaries and filled spaces in between. In order to obtain a fiber of a given diameter and required structural parameters (distance between holes, hole diameter, core diameter) the intermediate perform is complemented by extra glass rods. Such an intermediate preform is then fused and drawn again with a fiber drawing tower to a final fiber with micrometer-scale structure. Finally, extra layers of polymer are usually added in this process to create a coating protecting the fiber mechanically. During the experiments it is observed that the thinning of a structure with a given symmetry affects the shape of the holes' cross-section. When the wall thickness is small, they tend to adopt a shape corresponding to the symmetry of the lattice. For a hexagonal lattice, it is a hexagon while for a square lattice it is a square. This is apparent when the thinning is applied to highly viscous glass (low temperature) and to structures with a high d/Λ (> 0.6) ratio (Fig 1.6f).

The same phenomenon is evident in the thinning of multi-fiber structures (image guides). Obtaining photonic fibers with required transmission characteristics is a difficult technological problem. One has to shape structures of microscopic size controlling only macroscopic parameters such as temperature and stretching rate. Defects are encountered affecting properties of the structure that deviate from their ideal values assumed in the simulations. The main fabrication problems are presence of deformed air holes, emergence of additional holes, and perturbations of the structure's symmetry (Fig 1.7). The presence of holes with different diameters and irregular shapes is clearly visible in structures with a square lattice. Usually the temperature in the fiber is non uniform and has a radial distribution.

As a result, the outer holes become more deformed and have smaller diameters. It is therefore recommended to add two or three rings of capillaries around the originally designed structure. Those additional capillaries do not affect the mode guided in the defect. Emergence of additional holes is often present when the spaces between capillaries do not close during the thinning process. Perturbation of the structure's symmetry is observed, especially in a square lattice, where holes may be displaced (tending to adopt triangular symmetry), the structure may be skewed or the rows of holes may be undulated. Avoiding such flaws requires a precise control of all thinning processes (capillaries, intermediate preform). It is essential to properly adjust and control the temperature of the thinning process, the temperature distribution in the oven, centering of the preform guidance, the speed of feeding and pulling. These parameters determine the diameter of the fiber, the temperature distribution over its cross-section and the heating time. Most reports on PCFs have described fibers made of silica glass. Silica provides very good fiber performance for most applications with wavelengths in the range of 200-2500 nm, but using other materials can enhance specific parameters of the fibers and transmission outside this spectral region [12].

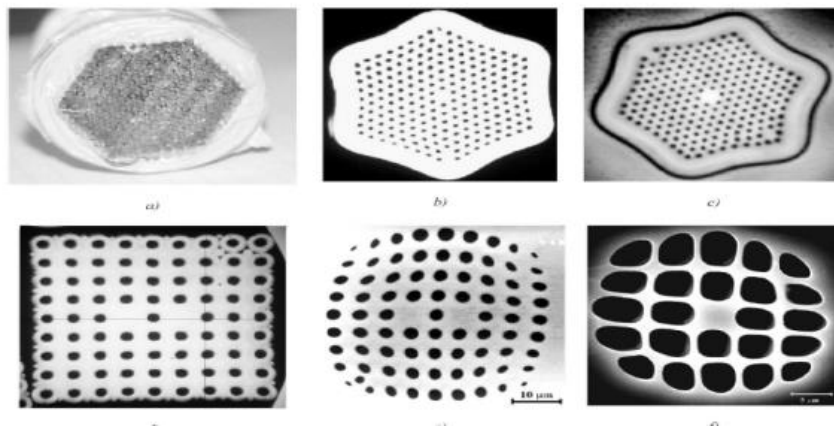


Fig 1.6. Fabrication of photonic crystal fibers: preforms, intermediate preforms and final fibers (Institute of Electronic Materials Technology (IEMT)): (a) the preform of PCF with holes $9 = 1$ mm with hexagonal lattice; (b) the intermediate preform with air holes $9 = 250$ (m with hexagonal lattice; (c) the PCF fiber; diameter of the fiber $9 = 120$ (m, air holes diameter $d = 3$ (m, $d/\Lambda = 0.5$; (d) the intermediate preform of double core PCF with square lattice; (e) a double core PCF fiber with a square lattice, diameter of the fiber 250 (m, air holes diameter $d = 2.5$ (m, $d/\Lambda = 0.5$; (f) a multimode PCF fiber with a square lattice; diameter of the fiber 160 (m, air holes diameter 3 μ m.

Most reports on PCFs have described fibers made of silica glass. Silica provides very good fiber performance for most applications with wavelengths in the range of 200-2500 nm, but using other materials can enhance specific parameters of the fibers and transmission outside this spectral region. Therefore, more and more attention is also paid to fibers drawn from

multi component glass: tellurite, fluoride, and chalcogenide ones. Multicomponent glass offers several useful properties not possessed by silica, such as a high refractive index, good infrared transmittance, high optical nonlinearity and relatively low photon energy. Several fibers made of silicate, chalcogenite, and tellurite glass have been reported. The silicate glass can be doped much more and therefore the range of possible modifications of their optical and mechanical characteristics is much wider. The high attenuation in glass of this type is usually considered to be a great disadvantage. However, this property is unimportant wherever short lengths of fiber are used, e.g. in sensors.

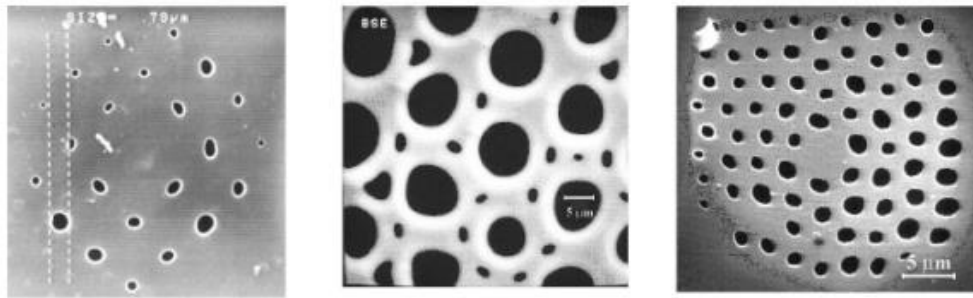


Fig 1.7. Defects in PCF fabrication: (a) the 5x 5 square structure with different hole diameters; (b) the hexagonal structure with gaps between capillaries not properly closed; (c) the 9x 9 square structure with displaced holes.

1.2.4 CATEGORIES OF PCF

There are two categories of PCF namely:

1. INDEX GUIDING FIBER

2. PHOTONIC BANDGAP FIBER

- PCFs can be categorized as Index guiding fiber and Photonic Bandgap Fiber. In High-index guiding fibers light is guided in much similar way as in conventional optical fibers but some modifications are there in PCFs guiding mechanism.
- In PCFs light is confined in solid core by a mechanism of Modified Total Internal Reflection. Refractive Index difference between core and cladding is positive but because of presence of air holes which causes lower refractive index.
- Refractive index of cladding is not constant but changes with wavelength. The group of wavelength which can pass through fiber is called modes while the group of wavelength which cannot pass or is blocked is called bandgap.

INDEX GUIDING FIBERS:

Index-Guiding Fibers have a solid core like conventional fibers. Solid-core PCFs guide light by Total Internal Reflection at the boundary between a low index cladding and a high index core. If the defect of the structure is realized by removing the central capillary, then guiding of an electromagnetic wave in a photonic crystal fiber can be regarded as a modified total internal reflection mechanism [13]. The modification is due to the network of air capillaries that leak higher modes so that only one fundamental mode is carried. This is the mode with the smallest diameter, close to the size of the defect, i.e., to the lattice constant of the periodic structure.

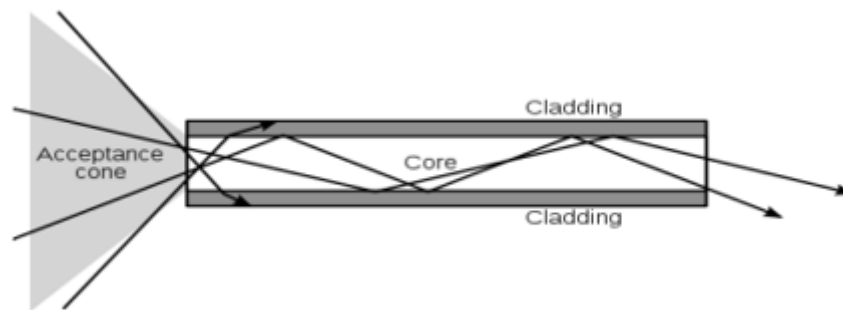


Fig.1.8 Index-Guiding Fibers

In this type of light guidance mechanism of PCFs, fiber cladding can be made of two dimensional photonic crystal with a core having higher refractive index than that of cladding. These fibers are also called as Index-Guiding. Fiber as difference in refractive index leads to the phenomenon of total internal reflection. Thus light travels through the fiber following a modified form of total internal reflection, called Modified total internal reflection. This leads to a property of endlessly single mode fiber where only fundamental mode is guided and multimode transmission is not possible.

SOLID CORE PCF:

- Like conventional fibers, solid-core PCF's guide light by Total Internal Reflection (TIR) at the boundary between a low index cladding and a high index core. In most all-solid fibers the required index difference is created by doping either the core or the cladding glass.

- In a PCF the same is achieved by incorporating holes into the cladding, causing the weighted average refractive index “seen” by the mode to be lower than that of the core.
- Similarly, it is easy to incorporate more than one core into the photonic crystal cladding, allowing one to form arrays of coupled or independent waveguide.

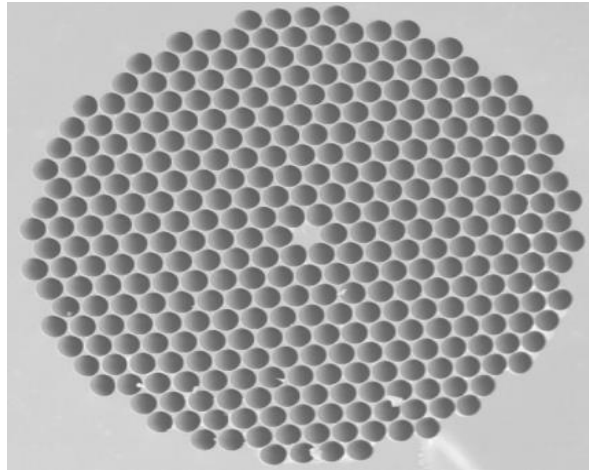


Fig. 1.9 Solid Core PCF

PHOTONIC BANDGAP FIBERS:

- Photonic crystal cladding have gaps for both positive and negative refractive index difference between core and cladding which leads to the formation of hollow core fiber with photonic crystal cladding having bandgap properties.
- The first PCF by exploiting Photonic bandgap effect to guide light was reported in 1998 having core with additional holes but could guide light in silica i.e. in higher refractive index.
- When white light was introduced in fiber core it showed that only limited wavelength range light was guided which coincide with photonic bandgap.
- Undoped silica glass is used for both core and cladding regions. Core is hollow(air).

- Constructive interference is produced by scattered light refracted at the core/cladding interfaces of the periodic lattice structure. Light can only propagate in specific regions.

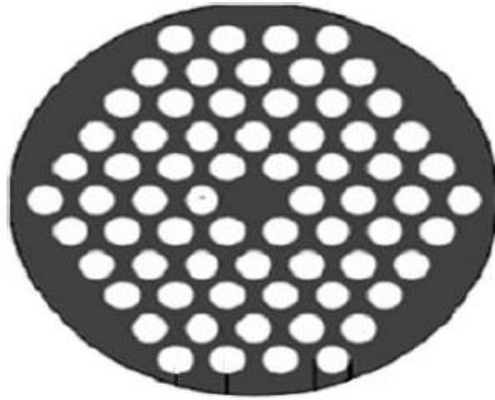


Fig. 1.10 Photonic Bandgap Fibers

HOLLOW CORE PCF:

- Hollow core fibers: Hollow core fibers employ a fundamentally different guiding mechanism.
- A photonic bandgap in the cladding acts as a virtually loss-free mirror confining light to a core that does not necessarily have to consist of solid material.
- This makes it possible to create low-loss waveguides with gas filled or even evacuated cores at optical wavelength.
- Photonic bandgaps can form in materials with a periodically structured refractive index [16].
- The fibers having core filled with air always having lower refractive index than that of cladding. In these fibers light propagate through the photonic bandgap mechanism.
- Since only a small part of light can be transmitted through glass, all effects related to interaction between glass and light like scattering, dispersion etc. are highly reduced .
- A hollow core with large diameter transmits about 99% of energy in air. By this the most common reason of attenuation is diminished.

- In hollow-core PCFs the main sources of attenuation are roughness of surfaces between core and cladding and size variation.
- As with conventional single mode fibers, the favored mode in hollow-core PCFs has a quasi-Gaussian intensity distribution.
- Unlike in conventional fiber where material dispersion plays a major role, group velocity dispersion (GVD) in hollow-core PCF is dominated by waveguide dispersion. A plot of dispersion versus wavelength is upward sloping and crosses zero close to the centre of the operating wavelength band, for any design wavelength, including those where the dispersion of silica makes it impossible to achieve zero dispersion in conventional fiber.

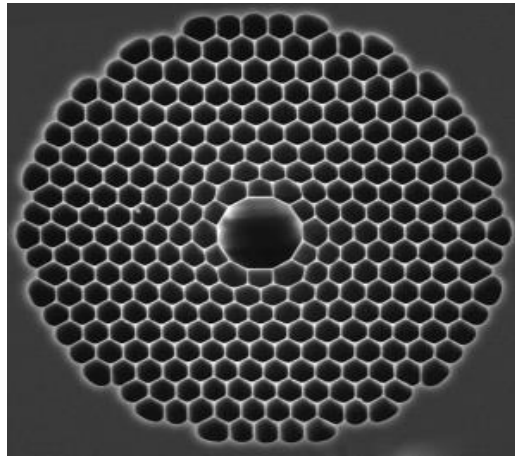


Fig. 1.11. Hollow core PCF

1.2.5. PROPERTIES OF PCF

REFRACTIVE INDEX:

The refractive index or index of refraction of a material is a dimensionless number that describes how light propagates through that medium. Using the Sellmeier's equation, pure silica is set as the background material of the fiber which refractive index changes according to the wavelength and followed by the equation.

$$n(\lambda) = \sqrt{1 + \frac{B_1 \lambda^2}{\lambda^2 - C_1} + \frac{B_2 \lambda^2}{\lambda^2 - C_2} + \frac{B_3 \lambda^2}{\lambda^2 - C_3}} \quad (1.19)$$

BIREFRINGENCE:

- The birefringence B is defined as a difference between the propagation constants β_x and β_y of the two orthogonal polarized components HE_x 11 and HE_y 11 of the fundamental mode:

$$B = \lambda(\beta_x - \beta_y) / 2\pi = |n_{effx} - n_{effy}| \quad (1.20)$$

- In photonic crystal fibers the birefringence obtained is highly insensitive to temperature. By slightly changing the air-holes geometry a wide range of birefringence can be obtained.
- The birefringence of the photonic crystal fibers is obtained due to non-axisymmetric distribution of the effective refraction index that depends on the size and spatial distribution of holes.
- Birefringent fibers, where the two orthogonally polarized modes carried in a single-mode fiber propagate at different rates, are used to maintain polarization states in optical devices and subsystems.

RELATIVE SENSITIVITY:

- Relative sensitivity coefficient r [12] can be expressed as

$$r = \frac{n_r}{Re[n_{eff}]} f \quad (1.21)$$

- Where n_r are refractive index of gas
- $Re[n_{eff}]$ is the real part of the effective mode index
- f is the fraction of the total power

$$f = \frac{\int_{holes} Re(E_x H_y - E_y H_x) dx dy}{\int_{total} Re(E_x H_y - E_y H_x) dx dy} \quad (1.22)$$

- The *V number* is a dimensionless parameter which is often used in the context of step-index fibers.
- The *V number* can be interpreted as a kind of normalized optical frequency. (It is proportional to the optical frequency, but rescaled depending on waveguide properties.) It is relevant for various essential properties of a fiber

$$V_{eff} = \frac{2\pi\Lambda}{\lambda} \sqrt{n_{co}^2 - n_{cl}^2} \quad (1.23)$$

- It must be less than 2.405 for the fiber to be single mode, where λ is the operating wavelength, a is the core radius, n_{co} is the core index, and n_{cl} is the cladding index.

EFFECTIVE AREA:

- E is the effective area of the fundamental mode is a measure of the area over which the energy in the electric field is distributed.
- A_{eff} in a single mode optical fiber determines how much energy the core can carry without causing non-linear type signal losses. This parameter is important for DWDM applications.

$$A_{eff} = \frac{(\iint |E|^2 dx dy)^2}{\iint |E|^4 dx dy} \quad (1.24)$$

NON – LINEARITY:

- The high intensity of core by strongly confining light enhances the nonlinearity property of fibers. Moreover different non-linear effects can also be achieved by proper design of dispersion characteristics.
- PCF is a very promising medium for super-continuum generation. Super-continuum Generation is a result of several different non-linear phenomena including soliton transmission. Soliton transmission requires balanced non-linear and dispersion characteristics which are obtained by modifying air-holes.
- Super-Continuum is the generation of continuous broad spectra of high power pulse when transmitted through non-linear media.

$$\gamma = \left(\frac{2\pi}{\lambda} \right) \left(\frac{n_2}{A_{eff}} \right) \quad (1.25)$$

- The effective nonlinear coefficient is a coefficient for quantifying the strength of a nonlinear interaction in the context of nonlinear frequency conversion.

CONFINEMENT LOSS:

The losses in PCFs occur for a number of reasons, such as intrinsic material absorption loss, structural imperfection loss, Rayleigh scattering loss, confinement loss, and so on.

Fabrication related losses can be reduced by carefully optimizing the fabrication process . Confinement loss is an additional form of loss that occurs in single-material fibers. PCFs are usually made from pure silica, and so the guided modes are inherently leaky because the core index is the same as the index of the outer cladding without air holes. This confinement loss can be reduced exponentially by increasing the number of rings of air holes that surround the solid core, and is determined by the geometry of the structure. It is important to know how many numbers of rings of air holes are required to reduce the confinement loss under the Rayleigh scattering limit for practical fabrication process. The confinement loss of the fundamental mode has been computed from the imaginary part of the complex effective index, n_{eff} , using

$$\text{Confinement loss} = 8.686 \times 10^6 \times k_0 \times \text{Im}(n_{\text{eff}}) \quad (\text{dB/m}) \quad (1.26)$$

1.2.5. APPLICATIONS OF PCF

i) Dispersion compensation

For instance, more of the fiber installed were design to operate at 1.3 μm , but no transmission is A very interesting application of photonic crystal fiber is as dispersion tailoring devices which is preferred at 1.55 μm and this fiber has considerable dispersion at this wavelength. Photonic crystal fiber can be employed as dispersion compensation in order to eliminate or reduce the dispersion. As a general rule, the bigger the dispersion compensation, the smaller the PCF length. What distinguish PCF as dispersion compensation technique compare with other method, is the fact that the range at which the compensation is made in a PCF (zero dispersion) is broad compare with the other methods. This is especially important for WDM, where compensation must be done in a broad range.

ii) Polarization maintaining PCF

Birefringence in a optical fiber arises as a consequence of stresses generated in the fiber during the fabrication process. This anisotropy has a important effect in the transmission characteristics of the fiber. Birefringence can also be induce by bending and thermal effect. The net effect is the generation of different optical axes. Plane polarized light propagating along the fiber will be resolved into components along in theses axes and as they propagate at

different speeds. As result phases differences are created resulting in elliptically polarized light. Finally, this phases mechanism cause delays in the optical signal, and this is know as polarization mode dispersion. PMD becomes important at high transmission rate. Polarization maintaining PCF is emerging as a new competitor for traditional polarization maintaining fiber. One advantage of PCF is that they remains single mode and thus can transmit polarized light in a broad range of frequencies. Also PCF has shorter beat length than common PMF which reduces bend-induced coupling between polarization states and improve the extinction rate. PCF presents, more stable temperature coefficient of birefringence. PCF's find application in sensors gyroscopes and interferometers [2].

iii) Fiber lasers and amplifiers

Fiber amplifiers are one of the key components of modern telecommunication. Also fiber lasers are starting to be more and more important in medicine, spectroscopy, and industry. Compared to conventional solid-state lasers, the great advantage of fiber lasers is their outstanding heat dissipation capability. It results from the large ratio of fiber surface to volume in a long, thin gain medium. Beam parameters depend only on design of the fiber and its quality is not perturbed with thermal distortion. Such fibers can be pumped by multimode laser diodes and provide lasing/amplification action in a single mode. Conventional SIFs for lasers consist of core and double cladding made of different materials most typically with a polymer outer cladding. Efficiency of these devices is limited by core size, numerical aperture, and Raman scattering in doped silica. It results in limited output power that such a device can deliver. Double clad of PCF is made of silica with two photonic claddings with different properties. The inner cladding ensures a high numerical aperture and is surrounded with a web of silica bridges which are substantially narrower than the wavelength of the guided radiation. The rare-earth ion doping medium of a fiber laser such as Yb, Nd, Er, Er/Yb, Tm, Ho is introduced into the core of the PCF

iv) Photonic Crystal Fibers for Sensing Applications

Despite of its youth in the sensing field, PCFs have awakened the interest of many scientific groups due to their promising characteristics. The biggest attraction in PCFs is that by varying the size and location of the cladding holes and/or the core the fiber transmission spectrum, mode shape, nonlinearity, dispersion, air filling fraction and birefringence, among others, can be tuned to reach values that are not achievable with conventional optical fibers.

Additionally, the existence of air holes gives the possibility of light propagation in air, or alternatively provides the ability to insert liquids/gases into the air holes. This enables a well-controlled interaction between light and sample leading to new sensing applications that could not ever be considered with standard OFs. Due to PCFs diversity of features they introduce a large number of new and improved applications in the fiber optic sensing domain. In this section, the applications of PCFs in sensing fields will be detailed, dividing it in two subsections, depending on the parameter that is measured. These two subsections are physical sensors and bio chemical sensors, and each is divided in the several types of sensors.

PHYSICAL SENSORS

Physical optic sensors measure physical parameters such as temperature, curvature, displacement torsion, pressure, refractive index, electric field, and vibration. The measurement, monitoring, and control of these parameters are of vast interest for several applications. Physical sensors that assess strain/displacement, curvature/bend, transversal load, torsion, and temperature are of immense interest for structural health monitoring. Civil structures like buildings, piles, bridges, pipelines, tunnels, and dams need continuous monitoring with the purpose of controlling and preventing abnormal states or accidents at an early stage, in order to avoid casualties as well as giving maintenance and rehabilitation advice and physical fiber sensors are perfect for this purpose. Other physical sensors like pressure and refractive index find applications in fields such as medicine and bio chemistry, while electric and magnetic field fiber sensors are of enormous benefit for sensing at high voltages, since they provide an insulating link to high-voltage areas (not offered by conventional electric sensors) .

- **Refractive Index Sensors**

Refractive index is a fundamental material property. Consequently, its accurate measuring is crucial in many applications. In food or beverage industries, the monitoring of refractive index is part of the quality control, and the development of simple and compact refractometers is key. Optical fiber refractive index sensors are attractive, owing to their small size, flexibility in their design, immunity to electromagnetic interference, network compatibility, and the aptitude for remote and in situ measurements. FBGs writing in a threehole germanium-doped-core SCF were reported with a resolution of 3×10^{-5} and 6×10^{-6} around mean refractive index values of 1.33 and 1.4 . LPG-based devices offer high

sensitivity to the refractive index variations of the surrounding medium. Refractive index measurement within a solid core PCF inscribed with LPGs was reported, where the coherent scattering at the cladding lattice is used to optically characterize materials inserted into the fiber holes—liquid water to solid ice transition is characterized through the refractive index determination [7]. A high sensitive refractive index sensor based in LPGs inscribed in an ESM PCF was reported presenting a wavelength measured sensitivity of 440 nm/RIU and an intensity measured sensitivity of 2.2 pm/°C, presenting and water filled solid core PCFs an excellent sensitivity of $\sim 10^{-7}$ RIU within a index range of suitable characteristics for applications such as label-free bio sensing.

- **Temperature Sensors.**

Fiber optic sensor is one of the most required in the commercial market due to the high number of applications in so many areas like chemical and semiconductor industries, typical turbine areas etc. Consequently, temperature-based PCFs sensors were quickly developed aiming to produce new sensors with improved characteristics, mainly improved sensibility and stability. Studies to understand the influence of the geometry and the material quality in the Hi-Bi PCF sensitivity to temperature were developed. A polarimetric interrogation to this kind of Hi-Bi PCF showed a sensitivity of 0.136 rad/°C at 1310nm.

- **Vibration Sensors**

Parameters like vibration amplitude and frequency are extremely important to detect structural damages in rotor blades, aircraft fuselages, and wing structures, and so forth. Fiber optic sensors play a special role in this field due to their small size, immunity to electromagnetic interferences, and, in the case of using single material PCFs, high insensitivity to temperature variations. Only recently, vibration measurements using PCFs were demonstrated: by using a Hi- Bi PCF embedded in a glass-fiber-reinforced polymer for high sensitivity vibration measurements up to 50 Hz and by using a polarization maintaining PCF embedded also in a vibrations and with a sensitivity of ~ 0.253 dB/mm. In both fiber sensors, polarization glass polymer composite material showing reliable frequency and amplitude measurements of maintaining or Hi-Bi PCFs were chosen due to their negligible level to temperature-vibration cross coupling.

BIO CHEMICAL SENSORS

Optical fibers can be used for sensing of chemical and biological samples. OF-based sensors are advantageous for chemical and bio sensing due to their miniaturization, small size, flexibility, and remote capability, making fibers suitable for *in vivo* experiments, due to the fact that these waveguides are electrically passive, not representing a risk to patients, since there are no electrical connections to their body, and due to the ability for real-time measurement and the possibility to simultaneously measure several parameters. One approach for chemical/bio sensing is to provide the fiber end with a suitable indicator or a material that responds to the parameter of interest. Chemically sensitive thin films deposited on selected areas of optical fibers can influence the propagation of light in such fibers depending on the presence or absence of chemical/biological molecules in the surrounding environment. A wide range of optical sensors has been developed for selective biomolecule detection. Most of them have reliability issues as they employ very fragile antibodies as sensing elements. When compared to the conventional OFs, PCFs offer a number of unique advantages in chemical and bio sensing applications. Due to the presence of air holes running along its entire length, these fibers have a unique ability to accommodate biological and chemical samples in gaseous or liquid forms in the immediate vicinity of the fiber core or even inside the core. PCFs can be used simultaneously for light guiding and as a fluidic channel, leading to a strong light/sample overlap. Such channels can be further functionalized with biorecognition layers that can bind and progressively accumulate target biomolecules, thus enhancing sensor sensitivity and specificity. Due to PCFs core and cladding air holes small size and the high overlapping between sample and light, a very small fluid volume is required for sensing. Using PCFs the amount of volume needed is of the order of hundreds of nanoliters to tens of micro liters, while in conventional optics measurement techniques the volumes needed are of order of one to ten milliliters. The use of extremely small volume is of huge interest for chemical and biomedical applications, like analytes detection or protein/DNA recognition [7].

- **Gas Sensors**

Many industries produce gaseous emissions as a consequence of the processes they develop. Chemical processing, glass melting, metal casting, transportation, pulp and paper, and energy production industries all produce different amount and types of gaseous emissions. As so,

monitoring and control gas has become an increasingly important consideration in an ever broader global environmental awareness context. For other industries such as chemical, biochemical, and military ones, gas diffusion is as important parameter to analyze. Therefore, it is of enormous importance to develop gas sensing techniques that are selective, quantitative, fast acting, and not susceptible to external poisoning. To satisfy these requirements PCFs are employed, the air holes running the entire length of the fiber will act as micro-sized capillaries allowing gas diffusion to take place, and the whole process can be monitored. PCFs are very attractive for fast, real-time detection and measurement of simple gases. Even more, PCF technology is compatible with telecommunications systems and can easily exploit remote sensing and multiplexing [7].

- **Molecular Sensors**

A molecular sensor is based in a molecule that interacts with an analyte to produce a detectable change. Molecular sensors combine molecular recognition with some form of reporter so the presence of the guest can be observed. This kind of sensors is very important for applications such as biochemistry or biomedicine for which the detection of molecules like DNA, proteins and cancer cells are of huge importance, as it is the use of the lower sample volume possible. PCFs microstructured channels make these fibers very appropriate for such applications, given that they can be used to control the interaction between guided light and fluids located within the holes while simultaneously acting as a tiny sample chamber. Two big advantages can be obtained with these fibers: high overlapping between light and sample which is not possible with OFs or typical spectroscopy measurement techniques and the ability to perform the measurement with a very little volume sample, typically μL or less, that is much lower than in conventional spectroscopy (mL) [7].

- **DNA Sensors**

DNA analysis techniques are usually performed by immobilizing a single strand of DNA on a glass chip and checking the hybridization of this strand to its complementary. The glass surface needs a functionalization treatment in order that the binding of biological species takes place, and hybridization is later proved through the measurement of the fluorescence signal produced by the labeled sample. Introducing PCFs instead of glass chips can lead to a significant improvement of the sensitivity, with respect to the present technology. DNA sensors based in HC-PCFs were reported: by using a highly efficient evanescent-wave detection of fluorophore-labeled biomolecule in aqueous solutions positioned in the air holes

of the microstructured part of the PCF or by using 16mm long piece of functionalized HC-PCF incorporated into an optic fluidic coupler chip towards the capture of a specific single stranded DNA string by immobilizing a sensing layer on the microstructured internal surfaces of the fiber . Using solid core PCF Bragg grating the detection of selected single stranded DNA molecules was reported, being hybridized to a biofilm in the air holes of the PCF, measuring their interaction with the fiber modes . By using LPGs in an LMA PCF and immobilizing a layer of biomolecules on the sides of the holes of the PCF, the thickness of double stranded DNA was measured . A biosensor for DNA detection based in a three-hole SCF was demonstrated, by functionalization and selective detection of DNA through hybridization of immobilized peptide nucleic acid probes [7].

1.4. ORGANIZATION OF THE REPORT

First we will discuss the basics of PCF, then we discuss the chronological development of PCF, motivation of our work. In next chapter the basic equations for PCF is discussed first, then we discuss about the fabrication process, guiding mechanism of PCF. We also discuss about different types of PCF and different applications of photonic crystal fiber (PCF). The analysis method of our work is also discussed. Here we discuss about FEM method, COMSOL, the procedure of analysis using this software. In the last, our thesis outcome is described and finally the future scope of this work is discussed.

2. PROJECT DESCRIPTION AND GOALS:

2.1 METHODOLOGY:

A finite element based optical mode solver is the most popular method to rigorously analyze photonic crystal fibers. Since the introduction of the photonic crystal fiber (PCF), various wave guiding structures that utilize the arrangement of microstructured holes or thin layers have been realized. The large variety of possible hole shapes and arrangements demand the use of numerical methods that can handle arbitrary cross-sectional shapes to analyze this kind of structures. Besides, the existence of interfaces with high index-contrast between the solid host material and air holes calls for the use of the vectorial wave equation to accurately model the structure. Finite element method (FEM) is suitable for such analysis as it can handle complicated structure geometries and solve vectorial equations transparently.

2.2 Formulation

Using FEM, any waveguide structure can be analyzed in a relatively small computational domain for its complex-valued modal indices and field profiles. The structures being considered may include those with either solid material or air as the core; circular or noncircular microstructured holes arranged around the core. Through the FEM results, we have studied the leakage loss, dispersion properties, vectorial character, as well as the degeneracy of modes and single modeness of particular kinds of PCFs.

2.3 Boundary Conditions

During the numerical analysis, we have considered three types of boundary conditions. They are

Perfect Electric Conductor (PEC) :This boundary condition can be expressed as,

$$\mathbf{n} \cdot \mathbf{B} = 0 \quad (2.1)$$

$$\mathbf{n} \times \mathbf{E} = 0 \quad (2.2)$$

Here, \mathbf{n} is the unit normal vector to the boundary. According to this condition, tangential components of \mathbf{E} and normal components of \mathbf{B} is continuous across any interface.

Perfect Magnetic Conductor (PMC) :This boundary condition can be expressed as,

$$\mathbf{n} \cdot \mathbf{D} = 0 \quad (2.3)$$

$$\mathbf{n} \times \mathbf{H} = 0 \quad (2.4)$$

According to this condition, tangential components of \mathbf{H} and normal components of \mathbf{D} is continuous across any interface.

Perfectly Matched Layer (PML)

A perfectly matched layer is an artificial boundary condition implying perfect absorption of incident electric field. This boundary condition is required for approximating infinite zone beyond the waveguide outer edge to a finite domain of numerical analysis. Effect of PML on numerical solutions obtained will be more prominent when confinement of field in the PCF is weak. This layer can also be utilized to find out the complex part of effective index. The PML region can be viewed as a perfect absorber with a certain magnitude of conductivity. However, the optimized conductivity is calculated from certain sets of equations. In our work, we have considered cylindrical PML available in the COMSOL software.

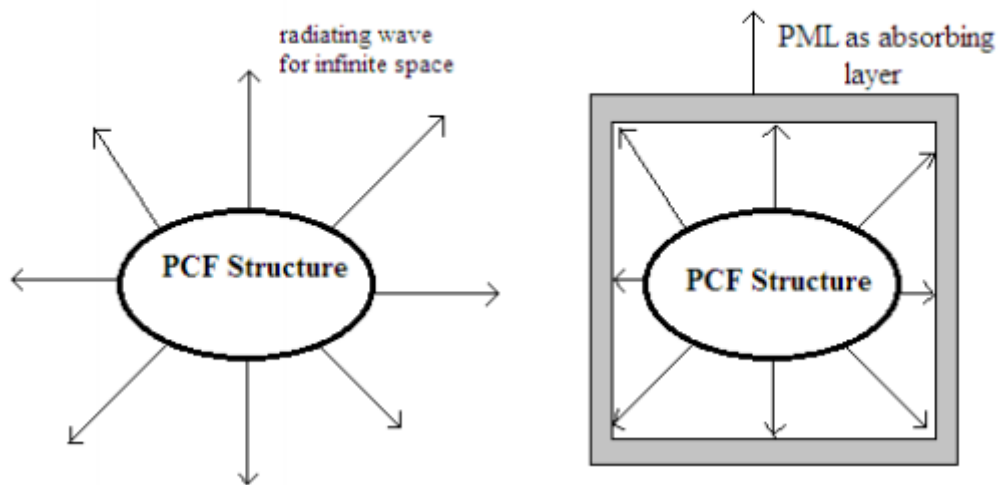


Fig 2.1(a). Schematic of a typical wave-equation problem, in which there is some finite region of interest where sources, inhomogeneous media, nonlinearities, etc are being investigated, from which some radiative waves escape to infinity. **2.1(b).** The same problem, where space has been truncated to some computational region. An absorbing layer is placed adjacent to the edges of the computational region—a perfect absorbing layer would absorb outgoing waves without reflections from the edge of the absorber.

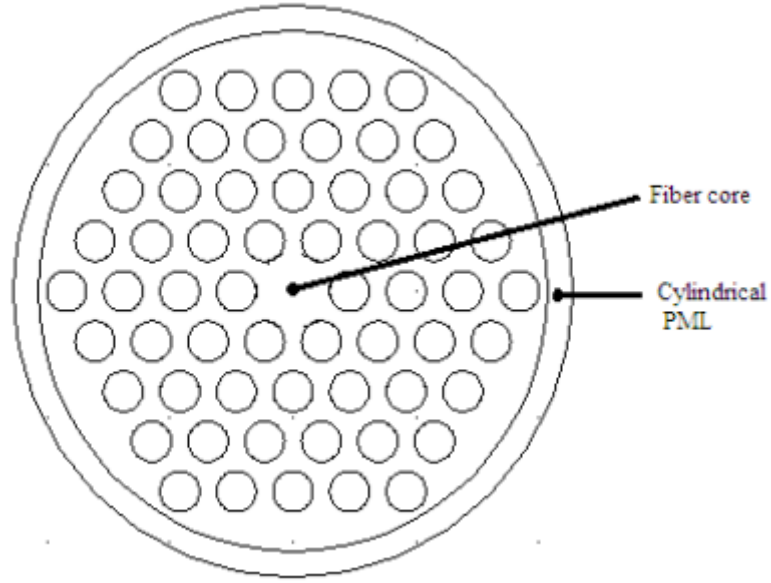


Fig 2.2. PML region surrounding the waveguide structure

Formulation of wave equations in the PML region can be done after rigorous analysis,

$$\Delta^{\wedge} \vec{H} = j\omega n^2 s \vec{E}$$

$$\Delta^{\wedge} \vec{E} = -j\omega \mu_0 s \vec{H}$$

$$S = 1 - (j \times \frac{\sigma_e}{\omega n^2 \epsilon_0}) = 1 - (j \times \frac{\sigma_m}{\omega \mu_0}) \quad (2.5)$$

Where E: Electric Field,

H: Magnetic Field &

σ_e and σ_m : Electric and magnetic conductivities of PML, respectively. s is the thickness of the PML layer which is ideally a multiple of the operating wavelength.

2.4 Comsol Mutiphysics

- We have worked with COMSOL MULTIPHYSICS software to check different properties of PCF. We have got our desired numerical answers & graphs of different parameters of spiral PCF using this software. Our COMSOL software version is 5.4.
- COMSOL Multiphysics (the name is meant to be an acronym of COMMon SOLution) is a cross-platform finite element analysis, solver and multiphysics simulation

software. It allows conventional physics-based user interfaces and coupled systems of partial differential equations (PDEs).

- COMSOL provides an IDE and unified workflow for electrical, mechanical, fluid, and chemical applications. An API for Java and Live Link for MATLAB may be used to control the software externally, and the same API is also used via the Method Editor.
- COMSOL contains an App Builder which can be used to develop independent domain-specific apps with custom user-interface. Users may use drag-and-drop tools (Form Editor) or programming (Method Editor). Specific features may be included from the model or new features may be introduced through programming.
- It also contains a Physics Builder to create custom physics-interfaces accessible from the COMSOL Desktop with the same look-and-feel as the built-in physics interfaces.

Here we describe the working procedures of our work using COMSOL with MATLAB.

3. TECHNICAL SPECIFICATIONS

3.1. Design of a PCF structure using COMSOL

- Open software **COMSOL 5.2**. A window named **Model Wizard** will be opened.
- Then we gone through the following steps: **2D Dimension>Wave Optics>Ewfd >Study>Mode analysis** application mode.
- We get the software opened.

To design the structure of a PCF first set it at appropriate modal analysis, then draw the structure of PCF and give input for geometrical properties, initialize mesh and then solve the structure. The procedure for this work is given below.

• Setting for appropriate modal analysis

- We Select **Properties** in the Physics menu to open the Application Mode Properties dialog box.
- For convenience we set the property Specify wave using to free space wavelength. This makes the wavelength available in the Application Scalar Variables dialog box instead of the frequency.
- In the Constants dialog box, we enter the names and expressions for the refractive indices.

• Geometry modeling

The easiest way to create the crystal geometry is using a array of geometry objects.

- We start by drawing a circle with the radius and the center at desired values.
- We select the circle and click the **Array** button. In the **Displacement** edit fields, type some value for the displacements in both directions and in the **Array size** edit fields, enter data.

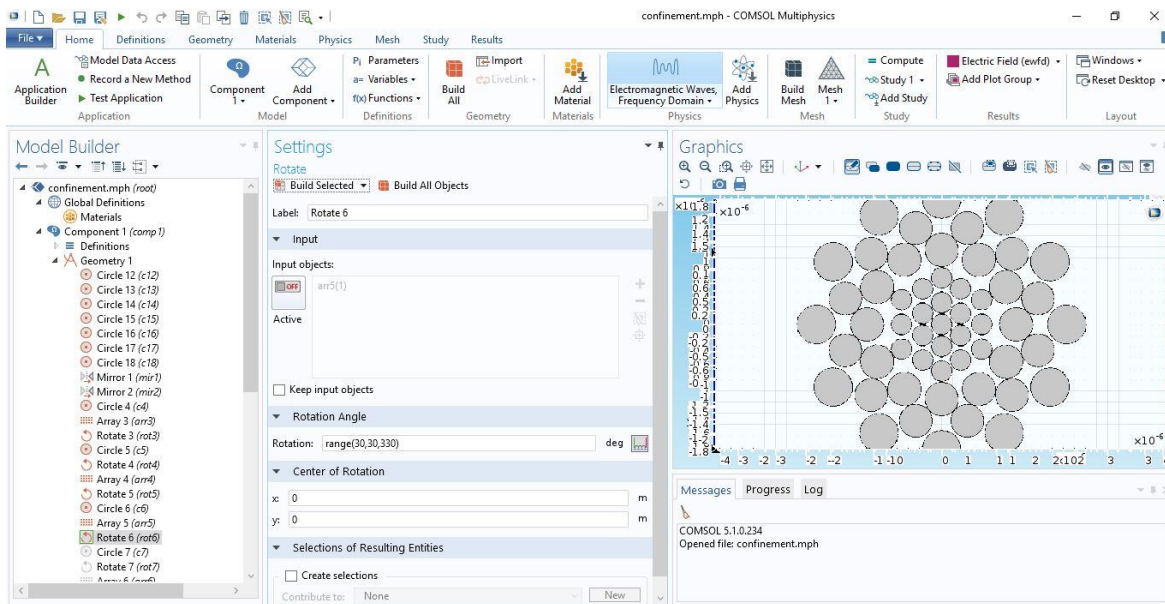


Fig 3.1 Design of a hexagonal PCF in COMSOL

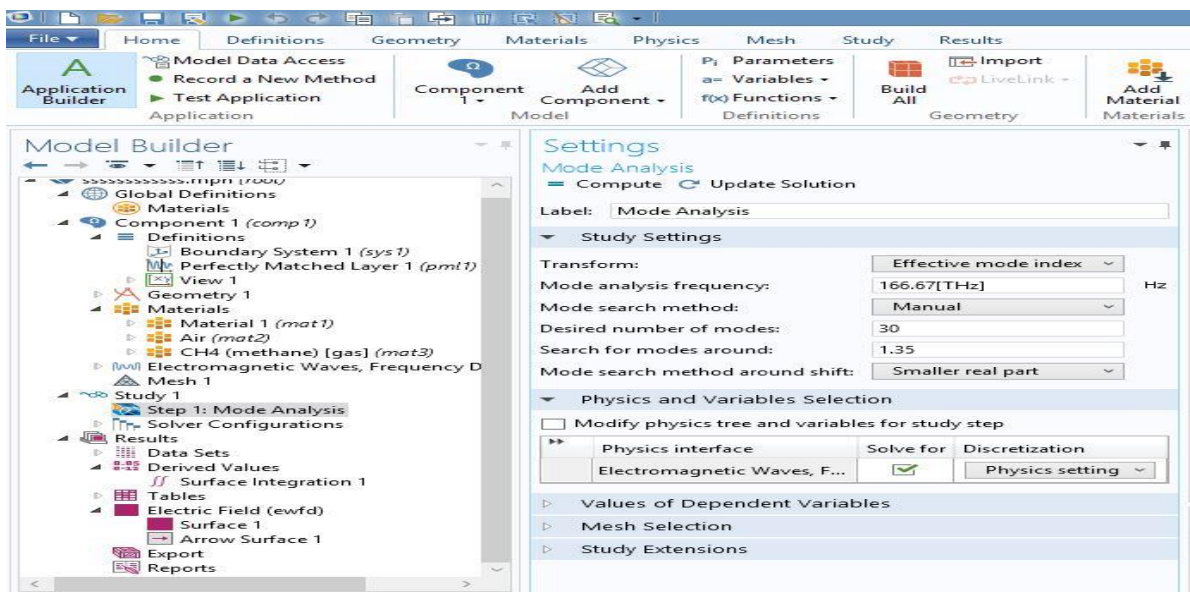


Fig 3.2 Modal Analysis of PCF

• Physics Settings

- In the Application Scalar Variables dialog box, we set the free space wavelength value. We will use the default boundary conditions on all exterior boundaries.
- In the Sub domain Settings dialog box we enter the refractive indices of different sub domains.

• Mesh Generation

- We then **initialize** the mesh.

- For more accuracy **refine mesh**.
- **Computing the solution**
 - In the Solver Parameters dialog box set the parameter Search for effective mode indices around to some value. This guarantees that the solver will find the fundamental mode, which has the largest effective mode index.
- **Post processing and visualizations**
 - In the **Plot Parameters** dialog box, we select surface and contour plots.
 - On the **Surface** page, we set the **Surface data** to **Electric field, z component**.
 - On the **Contour** page, we give **Magnetic field, z component** as **Contour data**.

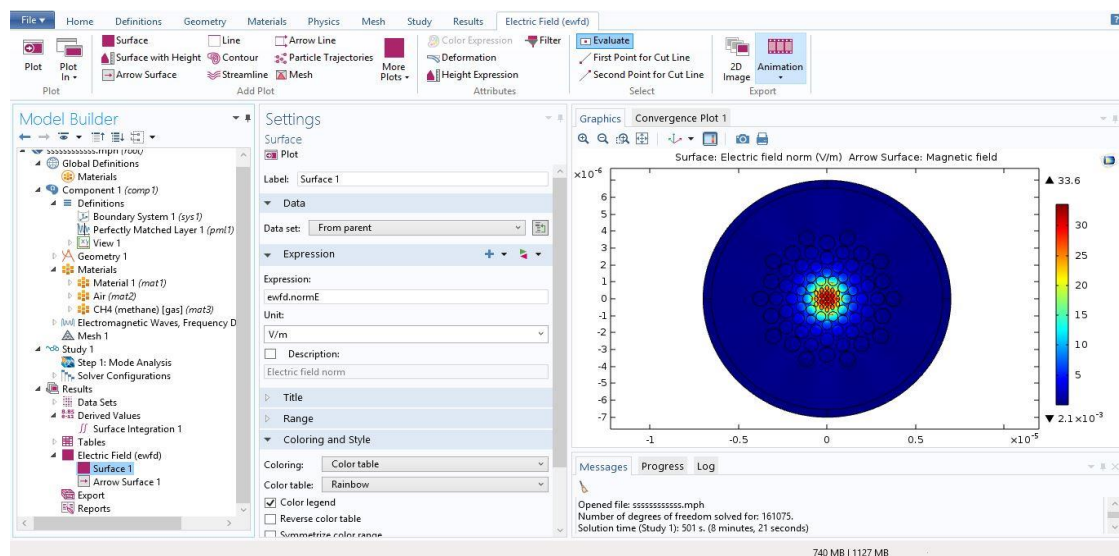


Fig 3.3 Power confinement shown in COMSOL window for a spiral PCF.

4. DESIGN APPROACH AND DETAILS

4.1. DESIGN APPROACH

A composed spiral PCF with the enhanced core region is designed. The cladding comprises of circular air holes in each spiral arm. Spiral cladding has been used in this design because of its exceptional modal confinement attributes. Spiral symmetry consists seven arms, where specific arm contains twelve air holes. Pitch is the middle to middle distance between neighboring gaps.

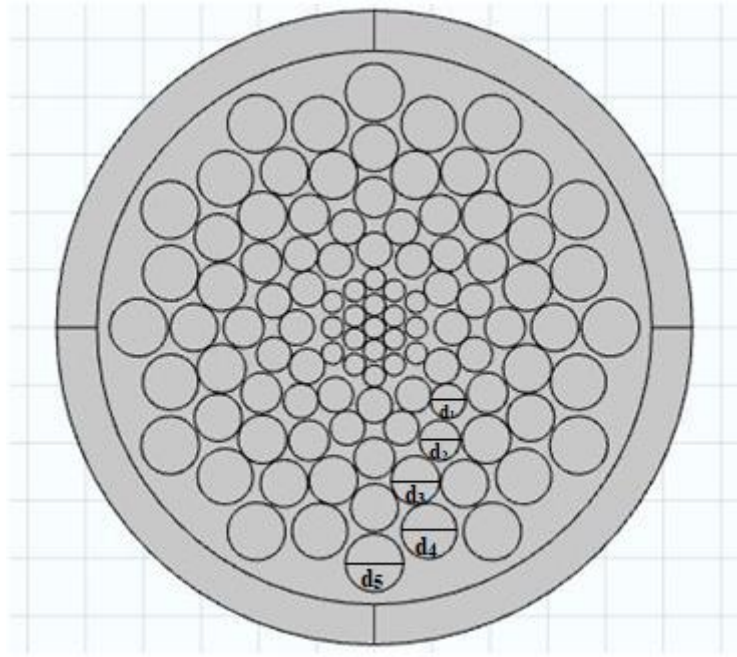


Fig 4.1 Schematic of the proposed S-PCF

For the design, pitch is defined as $r_0 = \Lambda$, where r_0 is the separation of the initial air hole in every spiral ring. Throughout the whole analysis, the value of Λ is set at $0.667 \times D_{\text{core}}$, where D_{core} presents the diameter of S-PCF core in μm unit. The air-hole distance across at

- initial two rings is given by $d_1 = d_2 = 0.45 \times \Lambda$
- third ring : $d_3 = 0.52 \times \Lambda$
- fourth and fifth rings : $d_4 = d_5 = 0.6 \times \Lambda$
- sixth ring : $d_6 = 0.7 \times \Lambda$
- seventh ring $d_7 = 0.74 \times \Lambda$.

The second air hole of each ring is fixed from the center by following the relation : $r_1 = r_0 + (0.35 \times \Lambda)$ distance. The measurement of the cladding air gaps should be as huge as conceivable with the goal that most of the light gets confined and reaches the core.

The suggested PCF contains ten air holes in each spiral ring which are arranged at a distance from the center with an angular displacement of $\theta_n = (n \times 360^\circ) / (2 \times N)$ where N denotes the number of circular rings. For example, angular distance of first ring is represented as $\theta_1 = (360^\circ) / (2 \times N)$. The optimized diameter d_c of the core region consists of the circular air holes as mentioned in the Fig 4.1. Throughout the analysis, air filling ratio of core is given by $d_c / \Lambda_c = 0.9$ which is kept as huge as possible in order to get high relative sensitivity. Hence, the proposed PCF exhibits high sensitivity and reduced confinement loss. The pitch between two neighboring circular air holes in the core is characterized as $\Lambda_c = 0.37 \times D_{core}$. Silica nanocrystal is selected as the background material whose refractive index varies according to the wavelength calculated by the Sellmeier's equation.

4.1.1. DESIGN SPECIFICATIONS :

$$\frac{d_c}{\Lambda_c} = 0.95 ; \Lambda_c = 0.42$$

$$d_c = 0.376$$

$$r_c = 0.188$$

$$d_{core} = 2.016$$

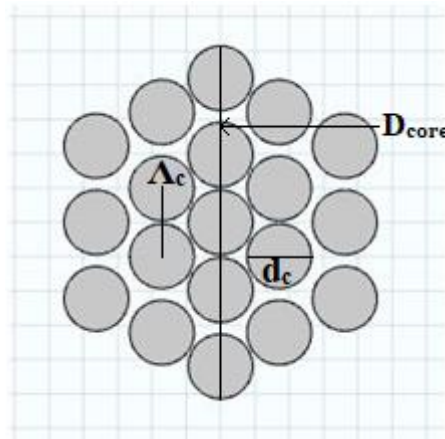


FIG 4.2 ENHANCED CORE OF S-PCF

$$\Lambda = 0.667 \times d_{\text{core}}$$

$$r_0 = \Lambda = 1.3455$$

$$r_{n+1} = r_n + (0.35 \times \Lambda)$$

$$r_1 = 1.8$$

$$r_2 = 2.2609$$

$$r_3 = 2.7411$$

$$r_4 = 3.1213$$

$$r_5 = 3.6515$$

$$r_6 = 4.0817$$

The radii of the air holes in the layers of the cladding can be calculated by:

$$\frac{d_1}{\Lambda} = \frac{d_2}{\Lambda} = 0.45$$

$$\frac{d_3}{\Lambda} = 0.52$$

$$\frac{d_4}{\Lambda} = \frac{d_5}{\Lambda} = 0.6$$

$$\frac{d_6}{\Lambda} = 0.7$$

$$\frac{d_7}{\Lambda} = 0.74$$

Where d_n denotes the diameter of the circular air hole in the cladding and n represents the layer of the cladding.

To simulate the optical properties of this proposed S-PCF, a finite element method (FEM) is used for solving Maxwell's equation. It can solve very complex structures and offer full

vector investigation of various PCF structures. It is known that due to the finite number of air holes in the cladding, light can leak among the air holes, which is called the leakage loss or confinement loss. So, to compute the leakage loss, an effective boundary condition is needed that produces no reflection at the boundary. In this case, Perfectly Matched Layers (PMLs) are the most efficient absorption boundary condition for this purpose. After the geometry of the proposed S-PCF is completed, a mesh is built.

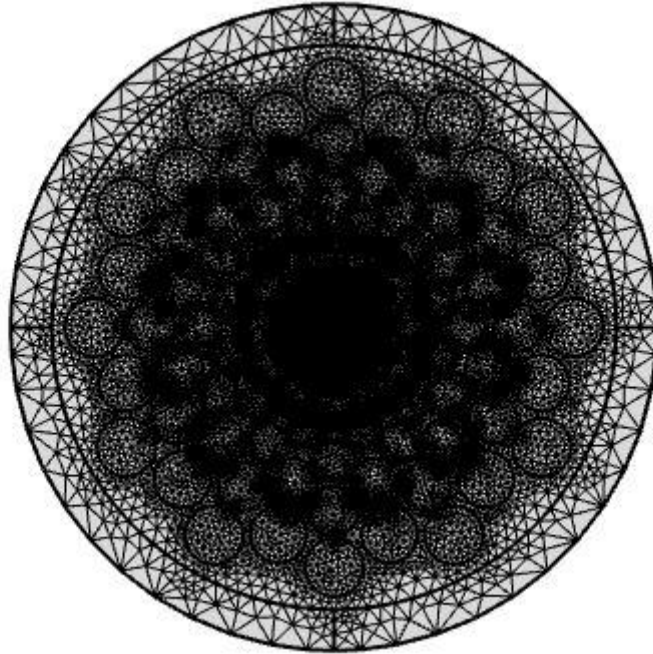


Fig 4.3 Built Mesh of the proposed S-PCF

The intensity distribution is observed using mode analysis. Modal intensity distribution along x and y polarization is observed.

4.1.2. Power Confinement

To analyse the guided mode of any PCF its first needed to check the power confinement of the structure which means whether it has guided mode or not. So, in our thesis we first check the power confinement at different wavelength for fundamental mode and then find its other characteristics. Here in fig 4.4 power confinement for a hexagonal pcf is shown at 1.4 μm wavelength for two fundamental modes. At right hand side color variation (red for maximum, blue for minimum power) for power is shown. From this figure it is shown that maximum

power is passed through the core (the center circle is for analytical purpose, this is not air hole).from figure power confinement for fundamental x and y mode are almost same.

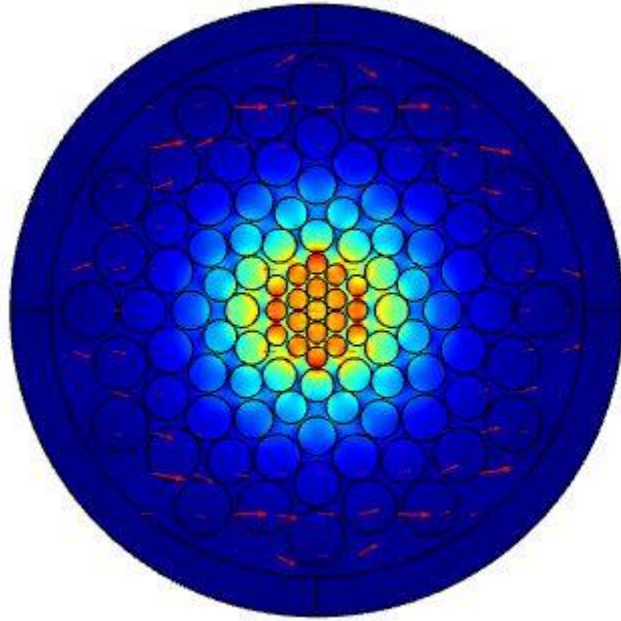
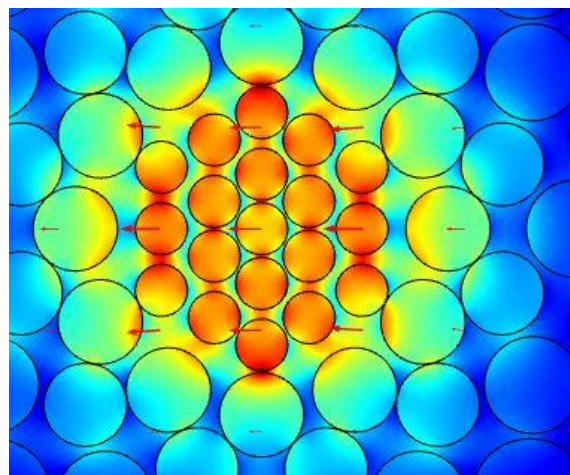


Fig 4.4. Power confinement for fundamental mode of a spiral PCF

4.1.3 ELECTRIC AND MAGNETIC FIELD FOR THIS PCF

Figure 4.5 shows the electric field vector of fundamental x and y mode for a PCF. Here field is shown by arrow sign. From figure it is clear that electric field vector distribution of the two fundamental modes are transversely related. On the other hand electric and magnetic field vector are also transversely related to each other and from our outcome this relation is verified.



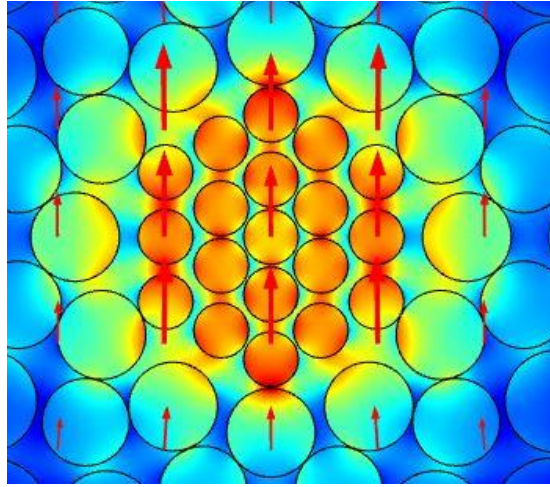


Fig 4.5. (a) E field for fundamental x mode. (b) E field for fundamental y mode.

4.2. CODES AND STANDARDS

IEC SMF Type B1.1

ITU Specification G.6522-The ITU-T G.652 fiber is the most commonly deployed single-mode fiber.

This standard SM fiber comes in four variants (A,B,C,D).

A and B have a water peak. C and D eliminate the water peak for full spectrum operation

TIA Specification TIA 492CAAA/OSI

4.3. CONSTRAINTS, ALTERNATIVES AND TRADE-OFFS:

- Problems related with Relative sensitivity has been solved by altering the design by changing the pitch between the core and the first ring of the cladding.
- High range of pitch in core causes Confinement issues in the design which can be overcome by varying $\frac{d_c}{\Lambda_c}$ ratio.
- The design of PCFs with high nonlinear coefficients due to its small effective area is more challenging. This was overcome by increasing air holes ratio in core.
- The diameters of the innermost ring are responsible for high sensitivity. We have chosen appropriate diameter to get high sensitivity

- The cladding air holes are optimized bigger to attain the low confinement loss and make the proper interaction of light through the core. All the parameters of both core and cladding were optimized by varying as a function of wavelength.
- For any smaller wavelength, the effective index of fundamental mode becomes real and Comsol Multiphysics considers the imaginary values beyond 10^{-10} range as negligible.

5. SCHEDULE, TASKS AND MILESTONES

S.NO	DURATION	WORK ALLOTTED
1	28/11/2017-20/12/2017	Objective and literature survey
2	2/1/2018 -31/1/2018	implementation of base paper
3	1/2/2018- 28/2/2018	designing new pcf structure
4	1/3/2018 - 25/3/2018	comparing results of various pcf structure
5	26/3/2018 - 6/4/2018	paper and report making
6	7/4/2018 -19/4/2018	poster making and final viva preparation

6. PROJECT DEMONSTRATION

6.1. PROPERTIES VARYING WAVELENGTH

• Effective index

The variation of effective refractive index of the fundamental mode of our hexagonal PCF is shown in fig.4.5. Using COMSOL with MATLAB interfacing here first $-j\beta$ can be found for a particular structure at a particular wavelength. The relation between β and effective index, n_{eff} is

$$\gamma = \left(\frac{2\pi}{\lambda}\right)\left(\frac{n_2}{A_{\text{eff}}}\right) \quad (6.1)$$

where λ_o is the operating wavelength and n_{eff} is the effective index of the PCF. From this equation effective index of the PCF can be found. From the figure effective index will be decreased with the increase of wavelength. Electromagnetic waves, Frequency Domain (ewfd) is observed for different wavelengths. Contour and arrow surface are also added for the ewfd results. E_x , E_y , H_x , H_y are the transverse electric and magnetic fields of the guided mode and are used for the surface integration process. These transverse fields and the effective index of mode n_{eff} can be calculated by solving Maxwell's equation by the process of FEM method. f is the fraction of the total power and is given by

$$f = \frac{\int_{\text{holes}} \text{Re}(E_x H_y - E_y H_x) dx dy}{\int_{\text{total}} \text{Re}(E_x H_y - E_y H_x) dx dy} \quad (6.2)$$

Beer-Lambert law is used to measure the absorbance of evanescent field by the gas samples. The relationship between gas concentration and optical field intensity is given by the following Eq. (2) which is given by the formula

$$I(\lambda) = I_o(\lambda) \exp(-r \alpha_m l_c) \quad (6.3)$$

Where, I and I_o are the output and input light intensities respectively, α_m is the absorption coefficient, l is the length of the S-PCF used for gas detection, c is the gas concentration, and r is a relative sensitivity coefficient defined by the equation given below. Refractive index of gas is given by n_r , $\text{Re}[n_{\text{eff}}]$ is the real part of the effective mode index and f is the fraction of the total power and is used for the calculation of relative sensitivity

$$r = \frac{n_r}{Re[n_{eff}]} f \quad (6.4)$$

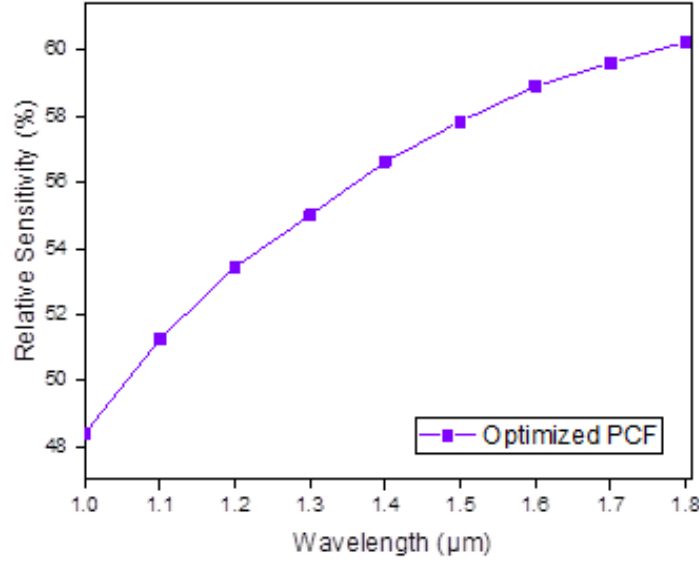


Fig 6.1 Relative sensitivity for a spiral PCF

• Confinement loss

Fig 6.2 shows the confinement loss of a hexagonal PCF with the variation of operating wavelength with the same pitch and hole pitch ratio. The confinement loss of the fundamental mode has been computed from the imaginary part of the complex effective index, using the equation.

$$\text{Confinement loss} = 8.686 \times 10^6 \times k_0 \times \text{Im}(n_{\text{eff}}) \quad (\text{dB/m}) \quad (6.5)$$

Confinement loss is defined by the energy of light which is permeable into the cladding region from the core due to finite number of air holes. The confinement loss can be denoted by L_c which is calculated through the visionary part of the refractive index n_{eff}

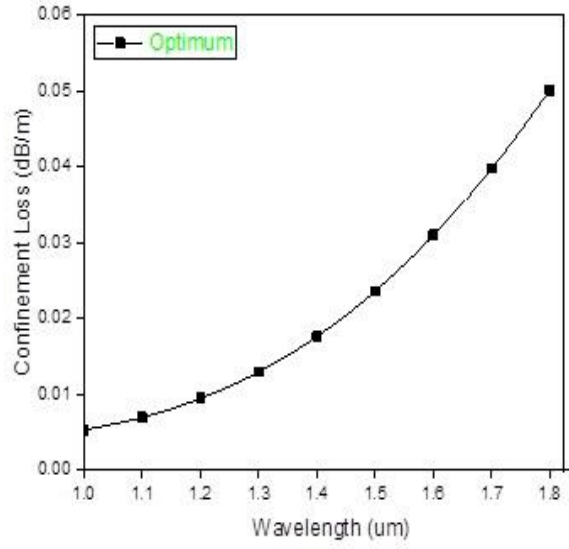


Fig 6.2. Confinement loss versus wavelength curve of the proposed S-PCF

• **V_{eff} parameter**

V_{eff} parameter for the S-PCF is used to verify the single mode behavior of the proposed structure. Multimode region is marked for $V_{eff} > 2.4$

It is given by

$$V_{eff} = \frac{2\pi\Lambda}{\lambda} \sqrt{n_{co}^2 - n_{cl}^2} \quad (6.6)$$

where $\frac{2\pi}{\lambda}$ denotes the wave number in the free space and Λ is pitch; n_{co} and n_{cl} represent the refractive index of core and cladding respectively.

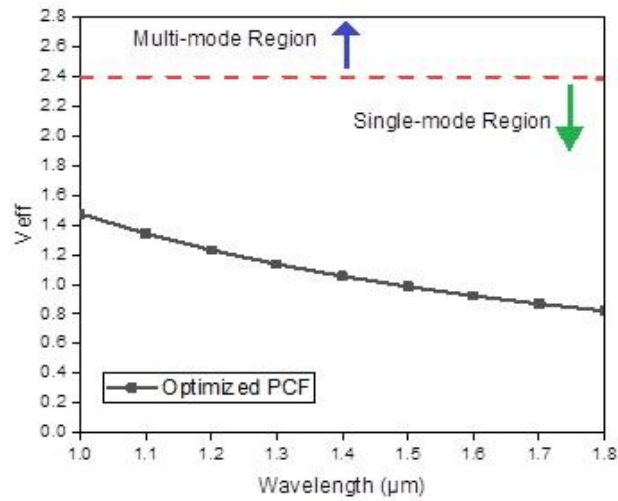


Fig. 6.3 V_{eff} vs wavelength for S-PCF

- **Effective Area and non-linearity**

Effective area of the fundamental mode is a measure of the area over which the energy in the electric field is distributed and is denoted by E_{eff} in a single mode optical fiber determines how much energy the core can carry without causing non-linear type signal losses.

$$A_{eff} = \frac{(\iint |E|^2 dx dy)^2}{\iint |E|^4 dx dy} \quad (6.7)$$

The effective nonlinear coefficient is a coefficient for quantifying the strength of a nonlinear interaction in the context of nonlinear frequency conversion. The high intensity of core by strongly confining light enhances the nonlinearity property of fibers. Moreover different non-linear effects can also be achieved by proper design of dispersion characteristics.

$$\gamma = \left(\frac{2\pi}{\lambda}\right) \left(\frac{n_2}{A_{eff}}\right) \quad (6.8)$$

Where γ is a non-linear coefficient

n_2 is Kerr refractive index

A_{eff} is the effective area

λ is the wavelength

Besides, it can be contemplated that by increasing the diameter of core and reducing Λ_c , relative sensitivity is promoted.

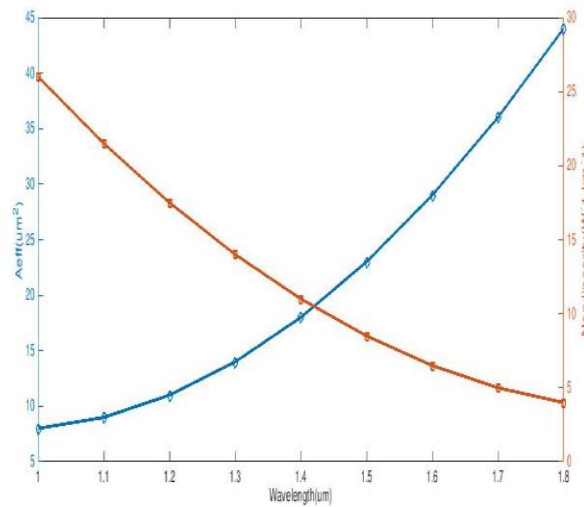


Fig 6.4 A_{eff} and non linearity versus wavelength

6.2. PROPERTIES VARYING PITCH

• n-effective

Effective index of a PCF will be changed with the change in pitch. Changes in effective index is shown for wavelength variation with different hole pitch ratio. Here blue line shows the effective index for $d/\Lambda=0.6$ and red line for $d/\Lambda=0.7$.

From figure if hole pitch ratio is increased the effective index will be decreased as the red curve is below the blue curve. On the other hand effective index will be increased with the increase of hole pitch. Here effective index is calculated at the operating wavelength $1.55\mu\text{m}$.

• A-effective

In Fig 6.4 effective modal area is shown with respect to pitch for different hole pitch ratio. Here two hole pitch ratio is considered. Blue curve is for the hole pitch ratio $d/\Lambda=0.6$ and red for $d/\Lambda=0.7$. From figure effective mode area can be tailored easily by changing pitch for different applications. For example, a large mode area can be useful in high power transmission [35]. Alternately, small mode areas can be useful for applications where the exploitation of the enhanced fiber nonlinearity is needed. So from figure a desired modal effective area can be found by changing the geometrical parameter.

• Confinement loss

In Fig 6.2 variation of confinement loss for different value of pitch is shown. Here blue curve indicates the variation of confinement loss for $d/\Lambda=0.6$ and the red curve for $d/\Lambda=0.7$. From figure confinement loss will be changed both for hole pitch and for d/Λ ratio. As the red curve is below the blue curve confinement loss will be decreased with the increase of d/Λ ratio. On the other hand with the increase of hole pitch confinement loss will be decreased.

Fig. 6.5 shows the effect of air filling ratio d/Λ_c in core region keeping other parameters fixed. Besides, it can be contemplated that by increasing the diameter of core and reducing Λ_c , relative sensitivity is promoted.

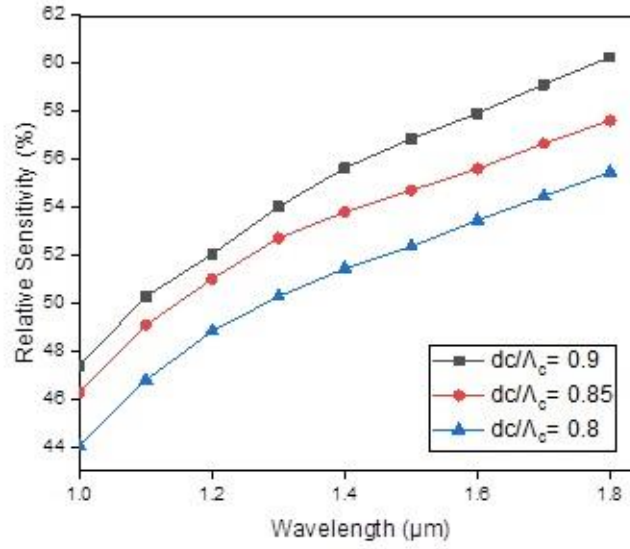


Fig.6.5. Relative sensitivity versus wavelength for the proposed S-PCF for the variation of filling ratio of the core

$\Lambda = 1.3455 \mu\text{m}$; $\Lambda_c = 0.395 \mu\text{m}$; $d_1 = 0.61 \mu\text{m}$; $d_2 = 0.61 \mu\text{m}$; $d_3 = 0.7003 \mu\text{m}$.

d_c/Λ_c is varied for different values as 0.9, 0.85 and 0.8. At the wavelength of $1.33 \mu\text{m}$, the variation of d_c/Λ_c defined as 0.9, 0.85 and 0.8 the considered relative sensitivities are 54.34%, 52.3% and 50.07% respectively. By increasing diameter of air holes in core, more light is confined and hence power fraction of hole increases. Therefore, increasing d_c/Λ_c promotes higher relative sensitivity.

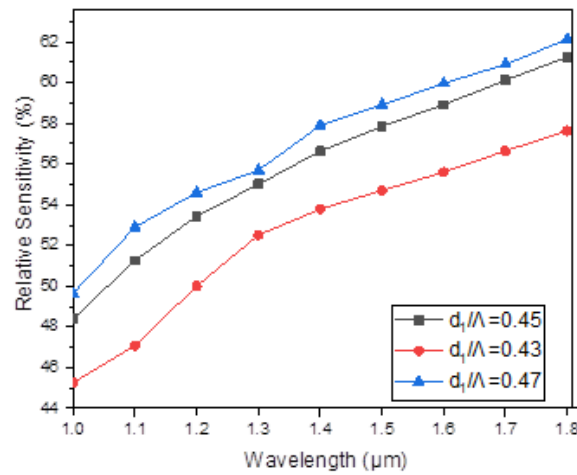


Fig.6.6. Relative sensitivity versus wavelength for the proposed S-PCF for the parameters: $\Lambda = 1.3455 \mu\text{m}$; $\Lambda_c = 0.395 \mu\text{m}$; $d_c = 0.376 \mu\text{m}$; $d_1/\Lambda = 0.45, 0.43$ and 0.47 , $d_2 = 0.61 \mu\text{m}$, $d_3 = 0.7003 \mu\text{m}$.

The diameter d_1 of cladding air hole is varied by keeping other parameters constant ($\Lambda = 1.3455 \mu\text{m}$; $\Lambda_c = 0.395 \mu\text{m}$; $d_c = 0.56 \mu\text{m}$; $d_2 = 0.61 \mu\text{m}$ and $d_3 = 0.7003 \mu\text{m}$) as shown in Figure 6.6. At the operating wavelength of $1.33 \mu\text{m}$, the variation of d_1 as 1.35 , 1.26 and $1.30 \mu\text{m}$ the air filling ratio in cladding is defined as $d_1/\Lambda = 0.45$, 0.43 and 0.47 the considered relative sensitivities are 55.1% , 52.9% and 56.2% respectively. By reducing the air filling ratio d_1/Λ , the transient field penetrating into field drops. Thus, the fraction power of holes depreciates and gives less absorption power in the core region. Hence, relative sensitivity reduces. On the other hand, if the air filling ratio is increased, the evanescent field confining into core region enhances which leads to increase in the fraction power of holes and hence relative sensitivity increases.

If the difference of the refractive indices between core and cladding drops due to air holes, most of the light passes through through the core and hence interaction between air and gas is increased. Therefore, sensitivity increases. To analyze the sensitivity of the proposed S-PCF efficiently, thickness of the outer layer is kept at 10% of fiber radius by PML test.

Full vectorial FEM with the perfectly matched layer (PML) boundary condition is one of the most potential numerical approaches obtainable to engineers for structuring and developing photonic elements and devices . To analyze propagation properties of leaky modes, the PML as boundary conditions is an essential technique in PCFs and by employing these layers, all optical propagation characteristics can be appraised in a single run. The PML depth of the fiber is 10% of the fiber radius is opted here.

All the parameters like Λ , d_c , d_1 and d_3 are kept constant. Figure 5.7 shows relative sensitivity curve when d_2/Λ is varied as 0.52 , 0.50 and 0.54 .The calculated relative sensitivities are 55.4% , 54.2% and 56.4% respectively at the operating wavelength of $1.33 \mu\text{m}$. By enhancing d_2/Λ , power fraction of holes rises and hence relative sensitivity increases.

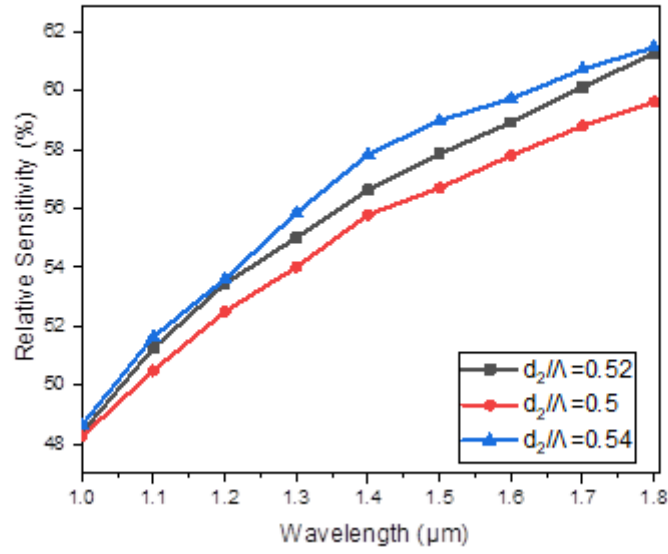


Fig.6.7. Relative sensitivity versus wavelength for the proposed S-PCF for the parameters: $\Lambda = 1.3455 \mu\text{m}$; $\Lambda_c = 0.395 \mu\text{m}$; $d_c = 0.376 \mu\text{m}$; $d_1 = 0.61 \mu\text{m}$; $d_2/\Lambda = 0.52, 0.50$ and 0.54 and $d_3 = 0.7003 \mu\text{m}$

The variation of d_3/Λ has been observed. Figure 6.8 exhibits variation of d_3/Λ on relative sensitivity for S-PCF. If d_3/Λ increases, evanescent field is strongly confined. in core region which will enhance power fraction of holes and hence relative sensitivity increases Diameter d_1 is more responsive to relative sensitivity than diameters d_2 and d_3 .

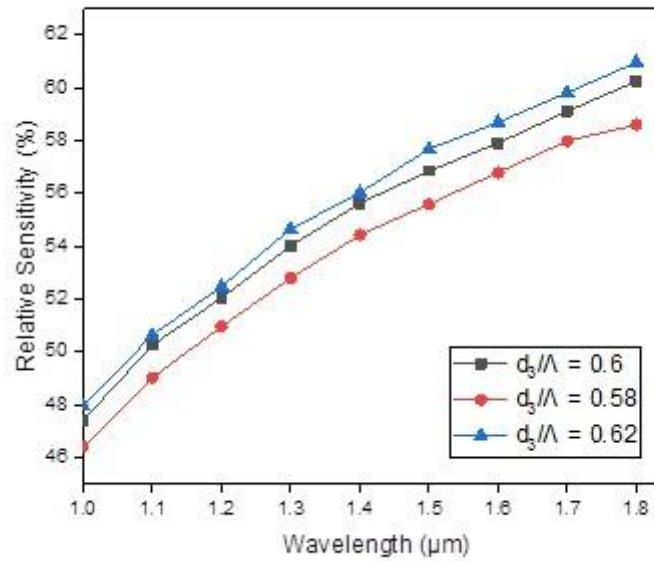


Fig.6.8. Relative sensitivity versus wavelength for the proposed S-PCF for the parameters: $\Lambda = 1.3455 \mu\text{m}$; $\Lambda_c = 0.395 \mu\text{m}$; $d_c = 0.56 \mu\text{m}$; $d_1 = 0.61 \mu\text{m}$; $d_2 = 0.61 \mu\text{m}$; $d_3/\Lambda = 0.6, 0.58$ and 0.62 .

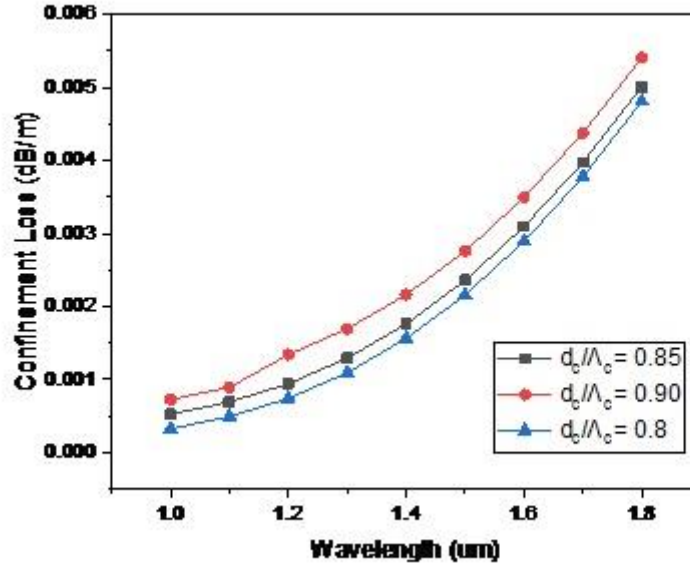


Fig.6.9. Confinement loss versus wavelength curve of the proposed S-PCF for optimized parameters: $\Lambda = 1.3455 \mu\text{m}$; $\Lambda_c = 0.395 \mu\text{m}$; $d_c = 0.376 \mu\text{m}$; $d/\Lambda = 0.92, 0.94, 0.90$

Confinement losses are the losses arising from the leaky nature of the modes and the non-perfect structure of the PCF fiber. Then, depending on the wavelength, number of holes rings, and hole size, modes will be guided with a structure dependent loss.

Finally, the manufacture procedure is one of the essential issues in PCFs. There are four different types of air holes which are utilized and delineated as shown in Fig1. A few techniques have been suggested for the fabrication of micro-structured strands like stack and draw, drilling, sol-gel casting and expulsion techniques. Be that as it may, the proposed structure can be created by latest innovation for mechanical progression in the creation of PCFs. Bise et al. gave a sol-gel method to create the PCFs with all structures and they give the opportunity to modify air-hole shape, spacing and size. In such circumstance, the sol-gel casting strategy gives plan adaptability and fabricates the suggested S-PCF. After drawing the relative sensitivity curve to the coveted level in the way just delineated, we can confirm the fidelity of the property of the proposed structure. A standard fiber draw, $\pm 1\%$ varieties in fiber global diameters may happen amid the manufacture procedure.

7. COST ANALYSIS

The cost of photonic crystal fiber varies depending on the design . Materials used for Core , Cladding and host material also plays an important role in determining the cost of PCF . Another major factor that should be kept in mind while determining the cost of PCF is fabrication techniques used in making PCF.

Price of some PCFs are given as follows:

F-SM15-PMEndlessly Single mode Photonic Crystal fiber , 15 μ m Core, PM: \$409/metre

F-SM5-PMEndlessly Single mode Photonic Crystal fiber , 5 μ m Core, PM : \$219/metre

8. CONCLUSION

A simple S-PCF as an optical sensor has been contemplated and examined that contains two layers permeable core with annular air holes. From above talks, it can be communicated that the relative sensitivity is enhanced by increasing the diameters of air holes situated at both cladding and center region and vice versa. The detailed S-PCF endeavors ultra-high relative sensitivity including birefringence between the wavelengths ranging from 1 μm to 1.8 μm . From analyzed results, it can be accounted for that the relative sensitivity and birefringence of the proposed S-PCF are around 57.08% and 7.53×10^{-3} individually at 1.55 μm wavelength. Moreover, the effective area and nonlinearity of 10.48 μm^2 and 13.97 $\text{W}^{-1} \text{km}^{-1}$ are accomplished separately at a similar wavelength. So, the proposed SPCF guarantees a noteworthy change for viable applications in lethal gas discovery including environment contamination monitoring.

In our proposed single core photonic crystal fiber design we have we have reviewed the analysis methods for numerical modeling in detail. Through the full-vector finite element method (FEM), the following fundamental characteristics of PCFs have been found out. Here we have found out that properties for both spiral and hexagonal lattice structure. The numerical method used here can be applied to designing not only index-guiding PCFs but also photonic band gap fibers. Numerical modeling techniques have great potential for designing profitable PCFs. The effects of the number of air holes and the geometrical parameters of the holes on the modal properties such as the confinement loss owing to the leakage nature of the modes and the effective area and how it is affected by approaching FEM modal analysis have been thoroughly detailed & explained.

We have verified our graphs and calculated numerical data's with given one's too .We have tried our best to keep our work in synchronization with the experimental proven one's .We have tried to cover all properties of single core fiber in our thesis work. However PCFs field is so vast that it was not possible for us to cover all the properties of it. Based on our work Dual core PCF & Multi core PCF structure can be constructed and their respective properties can be found out too. We have shown in our work that how maximum power can be obtained from fiber using the proper refractive index. We have shown how converging of Electric and Magnetic fields in the fiber core can be made possible. We have shown their field directions with arrow too. Our purpose of the work was to ensure how different loss mechanisms occurring frequently in fiber transmission can be minimized. We checked our work for two modes. One is fundamental x mode and the other is orthogonal y mode.

9. REFERENCES

- [1] S. Asaduzzaman, K. Ahmed, Proposal of a gas sensor with high sensitivity, birefringence and nonlinearity for air pollution monitoring, *Sensing and Bio-Sensing Research* 10 (2016)20–26
- [2] K.A. Stasiewicz, J.E. Musial, Threshold temperature optical fiber sensors, *Opt. Fiber Technol.* 32 (2016) 111–118.
- [3] S. Asaduzzaman, K. Ahmed, B.K. Paul, Slotted-core photonic crystal fiber in gas sensing application, *SPIE/COS Photonics Asia*, International Society for Optics And Photonics, October 2016, p. 100250O.
- [4] A.M. Pinto, M. Lopez-Amo, Photonic crystal fibers for sensing applications, *J. Sens.* 2012 (2012).
- [5] M. Morshed, M.I. Hassan, T.K. Roy, M.S. Uddin, S.A. Razzak, Microstructure core photonic crystal fiber for gas sensing applications, *Appl. Opt.* 54 (29) (2015) 8637–8643.
- [6] S. Olyaei, A. Naraghi, Design and optimization of index-guiding photonic crystal fiber gas sensor, *Photonic Sens.* 3 (2) (2013) 131–136.
- [7] M. Morshed, M.I. Hasan, S.A. Razzak, Enhancement of the sensitivity of gas sensor based on microstructure optical fiber, *Photonic Sensors* 5 (4) (2015) 312–320.
- [8] S. Asaduzzaman, B.K. Paul, K. Ahmed, Enhancement of sensitivity and birefringence of a gas sensor on micro-core based photonic crystal fiber, *IEEE 3rd Int'l Conf. on Electrical Engineering and Information & Communication Technology (ICEEICT)*, 2016, pp. 1–5.
- [9] S. Olyaei, A. Naraghi, Design and optimization of index- guiding photonic crystal fiber gas sensor, *Photonic Sens.* 3 (2) (2013) 131–136.
- [10] T.M. Monro, W. Belardi, K. Furusawa, J.C. Baggett, N.G.R. Broderick, D.J. Richardson, Sensing with microstructured optical fibres, *Meas. Sci. Technol.* 12 (7) (2001) 854.
- [11] S. Luke, S.K. Sudheer, V.M. Pillai, Tellurite based circular photonic crystal fiber with high nonlinearity and low confinement loss, *Optik* 127 (23) (2016) 11138–11142.

- [12] M.I. Hasan, M.S. Habib, M.S. Habib, S.A. Razzak, Highly nonlinear and highly birefringent dispersion compensating photonic crystal fiber, *Opt. Fiber Technol.* 20(1) (2014) 32–38.
- [13] W. Gao, Q. Xu, X. Li, W. Zhang, J. Hu, Y. Li, X. Chen, Z. Yuan, M. Liao, T. Cheng, X. Xue, Experimental investigation on super continuum generation by single, dual, and triple wavelength pumping in a silica photonic crystal fiber, *Appl. Opt.* 55 (33) (2016) 9514–9520.
- [14] N. Muduli, H.K. Padhy, An optimized configuration of large mode field area PMMA photonic crystal fiber with low bending loss: a new approach, *J. Mater. Sci. Mater. Electron.* 27 (2) (2016) 1906–1912.
- [15] R. Le Harzic, I. Riemann, M. Weinigel, K. König, B. Messerschmidt, Rigid and high numerical-aperture two-photon fluorescence endoscope, *Appl. Opt.* 48 (18) (2009) 3396–3400.
- [16] R.K. Gangwar, V.K. Singh, Study of highly birefringence dispersion shifted photonic crystal fiber with asymmetrical cladding, *Optik* 127 (24) (2016) 11854–11859. [26] R. Islam, S. Rana, Dispersion flattened low-loss porous fiber for single-mode terahertz wave guidance, *Opt. Eng.* 54 (5) (2015) 055102.
- [17] C. Zhao, Y. Wang, W. Qian, Y. Qiu, and S. Jin, “HiBi-PCF-FLM (fiber loop mirrors made of highly birefringent photonic crystal fiber) stress sensor strength detection differential demodulation and device,” China Patent, 2016.
- [18] J. Chen, R. Du, J. Hou et al., Multi-parameter sensor and system based on photonic crystal fiber, China Patent, 2010.
- [19] R. L. Willing, W. P. Kelleher, and S. P. Smith, “Photonic crystal interferometric fiber optical gyroscope system,” United States Patent, 2004.
- [20] H. Lehmann, H. Bartelt, R. Willsch, R. Amezcua-Correa, and J. C. Knight, “In-line gas sensor based on a photonic bandgap fiber with laser-drilled lateral microchannels,” *IEEE Sensors Journal*, vol. 11, no. 11, pp. 2926–2931, 2011.

- [21] R.K. Gangwar, V.K. Singh, Study of highly birefringence dispersion shifted photonic crystal fiber
- [22] B.W. Liu, M.L. Hu, X.H. Fang, Y.Z. Wu, Y.J. Song, L.Chai, C.Y. Wang, A.M. Zheltikov, High-power wavelength-tunable-photonic-crystal-fiber-based oscillator-amplifier-frequency-shifter femtosecond laser system and its applications for material micro processing, *Laser Phys. Lett.* 6 (1) (2008) 44.
- [23] S.P. Tai, M.C. Chan, T.H. Tsai, S.H. Guol, L.J. Chen, C.K. Sun, Two-photon fluorescence microscope with a hollow-core photonic crystal fiber, *Opt. Express* 12 (25) (2004) 6122–6128.
- [24] B.A. Flusberg, E.D. Cocker, W. Piyawattanametha, J.C.Jung, E.L. Cheung, M.J. Schnitzer, Fiber-optic fluorescence imaging, *Nat. Methods* 2 (12) (2005) 941-950
- [25] J.B. Jensen, L.H. Pedersen, P.E. Hoiby, L.B. Nielsen, T.P. Hansen, J.R. Folkenberg, J. Riishede, D. Noordegraaf, K. Nielsen, A. Carlsen, A. Bjarklev, Photonic crystal fiber based evanescent-wave sensor for detection of biomolecules in aqueous solutions, *Opt. Lett.* 29 (17) (2004) 1974–1976.
- [26] F. Fogli, L. Saccomandi, and P. Bassi. (2002, Jan.). Full vectorial BPM modeling of index guiding photonic crystal fibers and couplers. *Opt. Express* [Online]. 10(1), pp. 54–59.
- [27] Z. Zhu and T. G. Brown. (2002, Aug.). Full-vectorial finite-difference analysis of micro structured optical fibers. *Opt. Express* [Online]. 10(17), pp. 853–864.
- [28] G. E. Town and J. T. Lizer, “Tapered holey fibers for spot-size and numerical-aperture conversion,” *Opt. Lett.*, vol. 26, no. 14, pp. 1042– 1044, Jul. 2001.
- [29] J. T. Lizer and G. E. Town, “Splice losses in holey optical fibers,” *IEEE Photonic. Technology. Letter.*, vol. 13, no. 8, pp. 794–796, Aug. 2001.
- [30] N. Guan, S. Habu, K. Takenaga, K. Himeno, and A. Wada, “Boundary element method for analysis of holey optical fibers,” *J. Lightw. Technol.*, vol. 21, no. 8, pp. 1787–1792, Aug. 2003.

- [31] T.-L.Wu and C.-H. Chao, "Photonic crystal fiber analysis through the vector boundary element method: Effect of elliptical air hole," *IEEE Photon. Technol. Lett.*, vol. 16, no. 1, pp. 126–128, Jan. 2004.
- [32] M. Koshiba and K. Saitoh, "Numerical verification of degeneracy in hexagonal photonic crystal fibers," *IEEE Photon. Technol. Lett.*, vol. 13, no. 12, pp. 1313–1315, Dec. 2001.
- [33] S.S.A Obayya, B.M.A Rahman and K.T.V Grattan "Accurate finite element modal solution of photonic crystal fibres," *IEEE Proc. Optoelectron.*, vol. 152, no. 5, pp. 241–246, October 2005.
- [34] R. Buczynski, "Photonic Crystal Fibers," *Proceedings of the XXXIII International School of Semiconducting Compounds*, vol. 106, no. 2, January 2004.
- [35] Lara Scolari, "Liquid crystals in photonic crystal fibers: fabrication, characterization and devices." Ph.D. Thesis, March 2009.
- [36] D. Chen and M.-L. V. Tse and H. Y. Tam, "Optical Properties of Photonic Crystal Fibers with a fiber core of arrays of sub-wavelength circular air holes: Birefringence and Dispersion," *Progress IN in Electromagnetics Research*, Vol. 105, 193-212, 2010.
- [37] Ana M. R. Pinto and Manuel Lopez-Amo, "Photonic Crystal Fibers for Sensing Applications," *Journal of Sensors* ,Volume 2012, Article ID 598178, 21 pages, February 2012.
- [38] Joel Villatoro, Vittoria Finazzi, Gianluca Coviello, and Valerio Pruneri, "Photonic-crystalfiber-enabled micro Fabry Perot interferometer ,"*Optic Letters*", Vol. 34, No. 16, August 15, 2009.
- [39] A. Agrawal N.kejalakshmy , J Chen , B.M.A. Rahman and K.T.V. Grattan, "Soft glass equiangular spiral photonic crystal fiber for supercontinuum generation," *IEEE Photon .Technol.Lett* ,vol 21,no. 22, pp.1722-1724, Nov.15,2009.